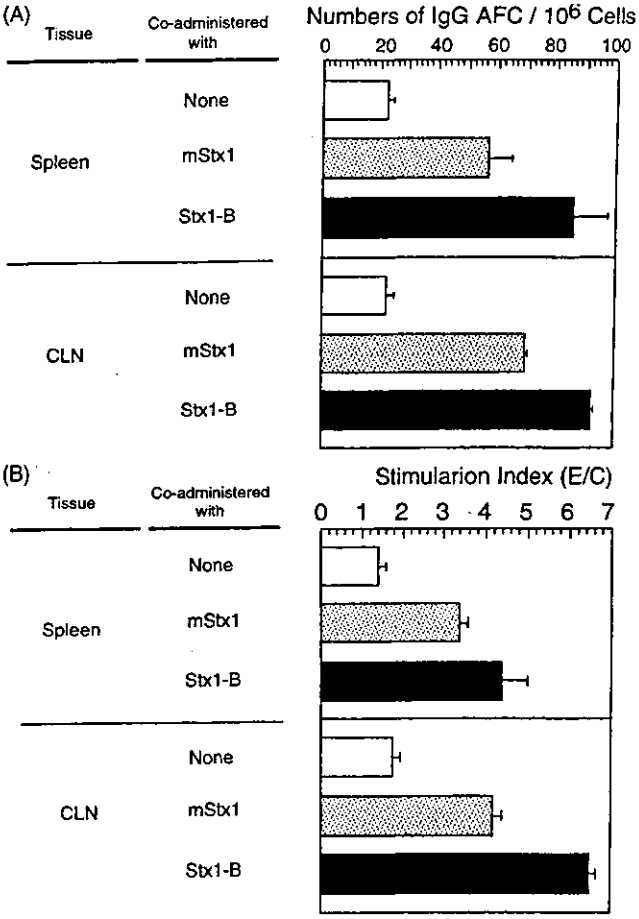

Fig. 2. Analysis of OVA-specific antibody-forming cells (AFC) and OVA-specific CD4$^+$ T cell proliferative responses in mice nasally immunized with OVA and Stx1 derivatives. Mice were nasally immunized with OVA (100 μg) plus 0.5 μg of mStx1 (dotted bar), 5 μg of Stx1-B (black bar) or OVA alone (white bar). Mononuclear cells were isolated from spleen of nasally immunized mice at day 21 and examined by Ag-specific ELISPOT (A). Purified splenic CD4$^+$ T cells were co-cultured at a density of 2×10^6 cells/ml with 1 mg/ml of OVA, T cell-depleted, irradiated splenic feeder cells (4×10^6 cells/ml) in the presence of rIL-2 (10 U/ml) in complete medium for 3 days for the proliferation assay (B). A control culture consisting of CD4$^+$ T cells, feeder cells and rIL-2 (10 U/ml) resulted in a [^{3}H] thymidine incorporation of 160 ± 19 cpm. The results are expressed as the mean of stimulation index ± S.E.M. from five to six mice per group and from a total of three experiments.

3.2. Ag-specific mucosal IgA immune responses induced by the co-administration of mStx1 or Stx1-B as a mucosal adjuvant

It is important to note that nasal co-administration of mStx1 or Stx1-B supported the induction of OVA-specific IgA Ab responses in mucosal secretions. Thus, nasal immunization with OVA and an optimal dose of mStx1 resulted in the induction of antigen-specific IgA Abs in saliva and nasal washes (Fig. 3A). Furthermore, co-administered Stx1-B also induced the secretion of OVA-specific IgA antibodies in saliva and nasal washes. In contrast, IgA Abs were not induced in mice by nasal immunization with OVA alone (Fig. 3A). Analysis of antigen-specific AFC further demonstrated that nasally co-administered mStx1 or Stx1-B supported the induction of OVA-specific IgA AFC in nasal passages and salivary glands (Fig. 3B). These findings further support the notion that the nontoxic Stx1 derivatives possess mucosal adjuvanticity for the generation of antigen-specific mucosal IgA responses following nasal administration.

3.3. Non-toxic Stx1-derivatives induced OVA-specific CD4$^+$ T cell responses

When CD4$^+$ T cells from spleen and CLN of mice nasally immunized with OVA plus mStx1 or Stx1-B were restimulated with the antigen in vitro, the levels of OVA-specific proliferative responses were increased (Fig. 2B). Antigen-specific CD4$^+$ T cell responses were the highest in mice nasally immunized with OVA and Stx1-B, and next highest in those immunized with OVA and mStx1. In contrast, there was virtually no Ag-specific proliferation in CD4$^+$ T cells isolated from mice given OVA alone (Fig. 2B). These results suggest that Stx1-B and mStx1 are potential adjuvants for the induction of antigen-specific CD4$^+$ T cells in both mucosal (e.g., CLN) and systemic (e.g., spleen) tissues.

In the subsequent experiment, the production of IL-4, IL-5, IL-6, IL-10 and IFN-γ production by antigen-specific CD4$^+$ T cells was analyzed at the protein level (Fig. 4). Increased levels of IL-4, IL-5, IL-6 and IL-10 production with low IFN-γ were seen in OVA-stimulated CD4$^+$ T cell cultures prepared from CLN and spleen of mice nasally immunized with OVA plus Stx1-B. Similarly, CD4$^+$ T cells isolated from mice nasally immunized with OVA and mStx1 also resulted in the induction of IL-4, IL-5, IL-6 and IL-10 production. Mice co-administered with Stx1-B always showed higher levels of Th2-type cytokine production than did those co-administered with mStx1. Splenic and CLN CD4$^+$ T cells from mice given OVA alone produced neither IL-4 nor IL-5, and only minimal amounts of IL-6 and IL-10. Taken together, these results show that nasal administration of OVA plus Stx1-B or mStx1 as mucosal adjuvant induced antigen-specific Th2-type cytokine responses which in turn led to the generation of OVA-specific mucosal IgA as well as predominant serum IgG1 Ab responses.

3.4. Up-regulation of co-stimulatory molecules and CD40 on NALT DCs following nasal application of Stx1-B or mStx1

To examine whether the increased Ag-specific Th cell and B cell responses seen in these nasally immunized mice were associated with NALT DC activation, we next analyzed the expression of costimulatory molecules, MHC class II and CD40 on NALT DCs by flow cytometry 24 h after nasal administration of naïve mice with Stx1-B or mStx1 (Fig. 5). Approximately 65–75% of NALT DCs isolated from non-treated mice constitutively expressed the

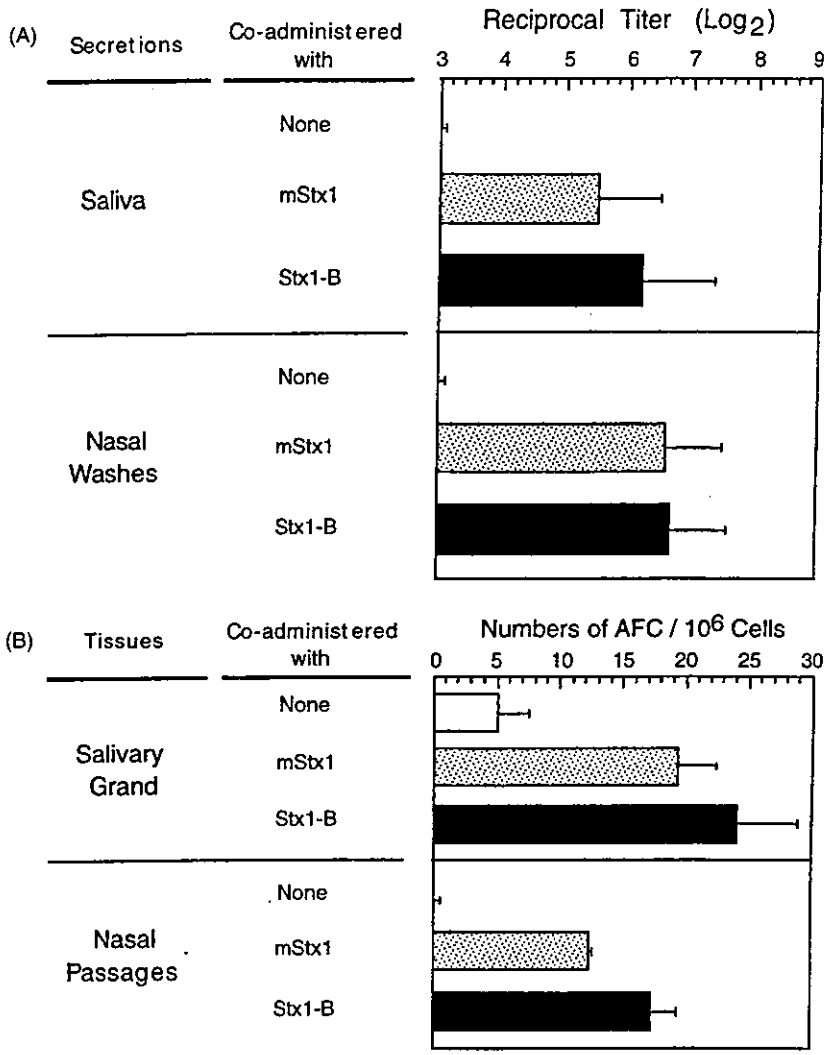

Fig. 3. Mucosal adjuvant activity of Stx1 derivatives for the enhancement of Ag-specific IgA responses. Induction of OVA-specific mucosal IgA Ab responses in saliva and nasal washes (A) and of OVA-specific IgA AFCs in salivary glands and nasal passages (B) of mice nasally immunized with OVA and mStx1 or Stx1-B was examined. Groups of mice were nasally immunized with OVA plus 0.5 μg of Stx1 mutant (dotted bar), 5 μg of Stx1-B (black bar) or OVA alone (white bar). External secretions were collected at day 21 and examined for OVA-specific IgA Ab responses by ELISA. Mononuclear cells were isolated from salivary glands and nasal passages of nasally immunized mice at day 21 and examined for OVA-specific IgA AFCs by ELISPOT. The results are expressed as the mean ± S.E.M. from five to six mice per group and from a total of three experiments.

co-stimulatory molecules CD80 and CD86 (Fig. 5). Further, most of these NALT DC expressed MHC class II (data not shown), with approximately 55% of cells positive for CD40. Following nasal administration of mStx1 or Stx1-B, the levels of CD80, CD86, and CD40 expression on NALT DCs were increased. These findings suggest that nasally co-administered mStx1 and Stx1-B trigger partially activated NALT DC to fully activate.

4. Discussion

In this study, we have assessed a mutant form of Stx1 (E167Q & R170L; mStx1) and the B subunit of Stx1 (Stx1-B) as possible mucosal adjuvants for the induction of antigen-specific mucosal and systemic immune responses. Nasal co-administration of non-toxic Stx1-B or mStx1 as mucosal adjuvant induced high levels of mucosal anti-OVA IgA as well as serum IgG anti-OVA Ab responses. These two distinct forms of non-toxic Stx1 derivative preferentially induced antigen-specific Th2-type $CD4^+$ T cells which in turn generated OVA-specific IgG1 and IgA antibodies in the systemic and mucosal compartments, respectively. Our finding that mStx1 and Stx1-B enhanced CD80, CD86 and CD40 expression on NALT DCs also supports the mucosal adjuvanticity of these two forms of non-toxic Stx1 derivative for the induction of antigen-specific immune responses.

If practical application of the mucosal adjuvanticity of these two forms of non-toxic Stx1 derivative is to be realized,

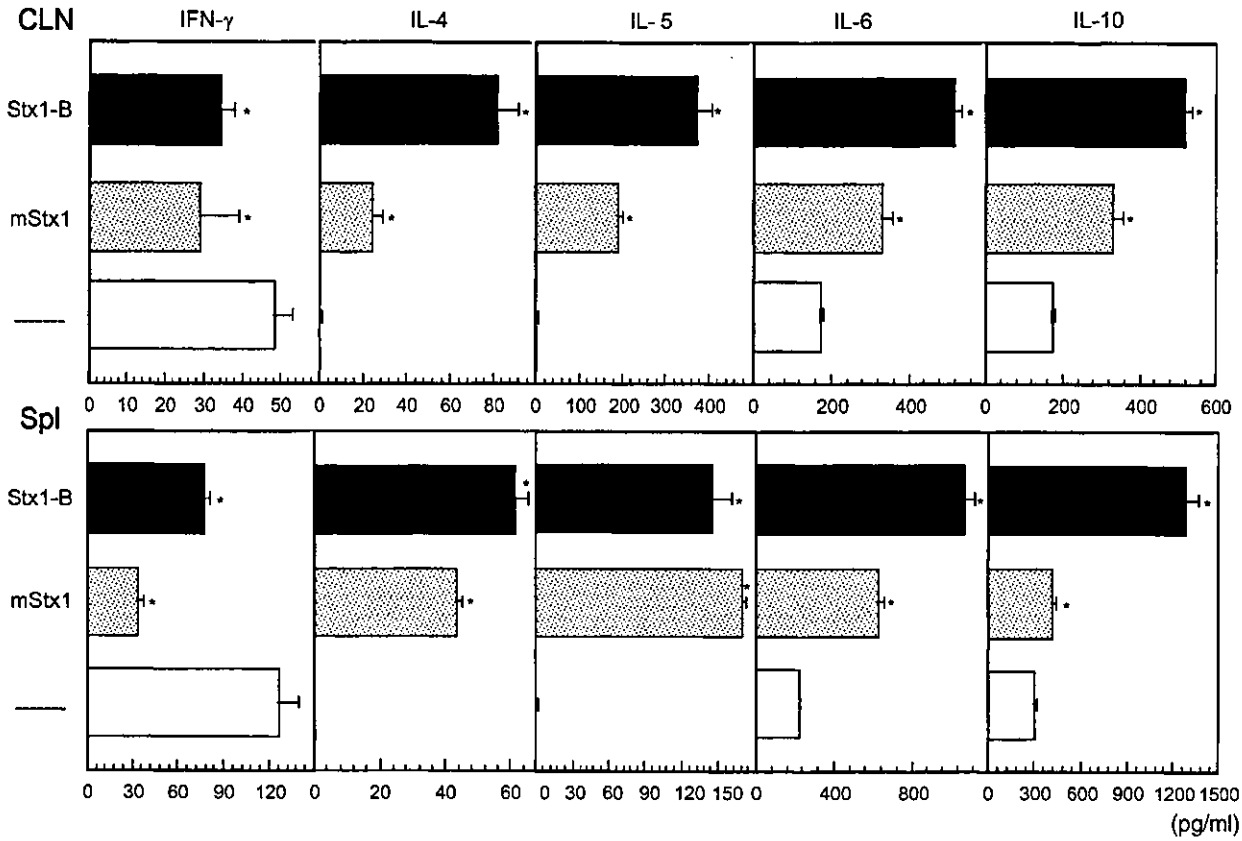

Fig. 4. Analysis of Th1 (IFN-γ) and Th2 (IL-4, IL-5, IL-6 and IL-10) cytokine synthesis by antigen-specific $CD4^+$ T cells isolated from mice nasally immunized with OVA and Stx1 derivative. $CD4^+$ T cells were isolated from CLN and spleen of mice nasally immunized with OVA plus 0.5 μg of mStx1 (dotted bar), 5 μg of Stx1-B (black bar) or OVA alone (white bar). Purified splenic $CD4^+$ T cells were co-cultured at a density of 2×10^6 cells/ml with 1 mg/ml of OVA, T cell-depleted, irradiated splenic feeder cells (4×10^6 cells/ml) for 5 days. Culture supernatants were harvested and then analyzed for cytokine secretion using the IFN-γ-, IL-4-, IL-5-, IL-6- and IL-10-specific ELISA. The results are expressed as the mean ± S.E.M. from five to six mice per group and from a total of three experiments. $^*P < 0.05$ when compared with mice immunized with OVA alone.

safety must be made a priority. The non-toxicity of these Stx1 derivatives had already been previously demonstrated by us both in vitro and in vivo studies. [18,28]. For example, our recent results showed that both native Stx1 (nStx1) and native Stx2 (nStx2) but not Stx1-B induced apoptosis in human monocytic THP-1 cells of eukaryotic cells [29]. Another our recent studies also suggested that nStx1 and nStx2 induced apoptosis in murine bone marrow (BM) cultures while both mStx1 and Stx1-B supported maturation and activation of DC from BM cultures (our unpublished data). As described above in Section 3, nStx1 possessed some nasal adjuvant activity at a dosage of 0.5 μg but proved lethal at higher doses (e.g., 2 μg). Moreover, mice given as little as 0.1 μg of nStx2 did not survive (data not shown). In contrast, all mice given a dose as high as 20 μg of mStx1 or Stx1-B as mucosal adjuvant survived and exhibited high levels of co-administered antigen-specific systemic IgG and mucosal IgA responses. Further, mice given doses as high as 20 μg of mStx1 or Stx1-B showed no sign (e.g., weight loss) of mucosal toxicity (data not shown). These findings further demonstrated the non-toxicity of mStx1 and Stx1-B as mucosal adjuvants.

When given nasally, mStx1 and Stx1-B supported the generation of antigen-specific $CD4^+$ Th2 type responses via the production of IL-4, IL-5, IL-6 and IL-10 and thereby enhanced Ag-specific serum IgG1 and mucosal IgA responses (Figs. 1 and 3). Based on these results, both of these nasally delivered non-toxic derivatives of Stx1 could be categorized as Th2 inducer type adjuvants. Although the exact mechanism by which these non-toxic Stx1 derivatives induce Th2-type T cell responses remains to be elucidated, it is interesting to note that such Th2-type T cell responses are also preferentially induced by oral or nasal administration of CT [4,30]. One obvious explanation would be that the tendency of a toxin-related adjuvant to favor Th1 and/or Th2 cell-mediated immune responses would be affected by the quality of antigen-presenting cells associated with mucosal compartments. For example, mucosally administered CT preferentially enhances B7-2-mediated Ag presentation by B cells and/or macrophages [31,32]. To this end, Th1 or Th2 polarizing factors could be mainly classified into three categories: (1) the anatomical and histological location of DC and T cells, (2) the nature of microbial products (adjuvant) and (3) the nature of the antigen used for the im-

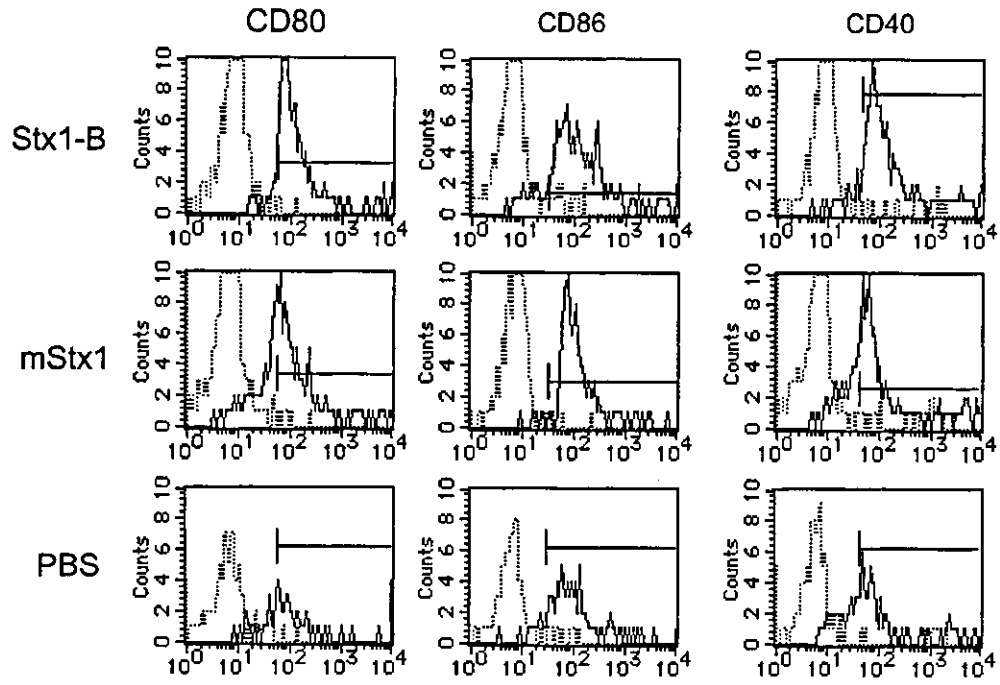

% of CD positive cells with high intensity

	CD80	CD86	CD40
Stx1-B	91.2 ± 7.6*	86.8 ± 3.2*	87.5 ± 1.0*
mStx1	80.8 ± 2.5*	93.9 ± 5.2*	74.7 ± 3.5*
PBS	73.5 ± 3.1	70.2 ± 5.1	56.5 ± 1.7

Fig. 5. Enhancement of CD40, CD80 and CD86 expressions on mucosal DC by nasal administration of non-toxic Stx1 derivatives. 24 h following nasal administration of an optimal dose of the Stx1 derivatives (0.5 μg of mStx1/mouse and 5 μg of Stx1-B/mouse), DC were examined by FACS to determine any alterations in CD40, CD80 and CD86 expression. The dotted line gives the background stain, omitting only the mAb used in the specific stain. Data are expressed as the mean ± S.E.M. and are obtained from a total of three independent experiments. *$P < 0.05$ when compared with control mice administered with PBS.

munization. For instance, the major T cell population in the lungs has been shown to be predominantly of the Th2 type [33], and Peyer's patches has been shown to be a site in which a high proportion of resting lymphocytes prefentially develop into Th2-type cells [34]. DCs in PP possess the ability to induce the differentiation of $CD4^+$ T cells into the Th2 pathway [35]. Thus, NALT DCs may also possess a similar ability to guide $CD4^+$ T cells to differentiate into Th2-type cells. Our data demonstrate that the expression of both CD80 and CD86 was enhanced on DC isolated from NALT of mice nasally administered with mStx1 or Stx1-B (Fig. 5). This pattern of co-stimulatory molecule expression suggests that mStx1- or Stx1-B-treated DC possess at least a capability for supporting Th2 type responses. Since PP, which along with NALT are the best- characterized mucosal inductive tissues, have been shown to contain three distinct subsets of DC including lymphoid, myeloid and double negative subsets [35], it is important to carefully examine the influence of the nasally administered Stx1 derivatives on different subsets of NALT DC and to determine the role of that influence in the creation of an environment conducive to Th2-type cell responses. To understand the importance of

the nature of the microbial compounds, one need only note that toxins such as CT and pertussis toxin have been shown to induce the development of DC type2 [36] and DC type1 [37], respectively, for the generation of Th2 and Th1 polarization, respectively [6,38]. In contrast, LT has been shown to support both Th1- and Th2-type responses [7]. Finally, the nature of the co-administered antigen itself may contribute to outcome of Th1 and/or Th2 polarization. Although CT is reported to be a potent Th2-inducing adjuvant, nasal vaccination with fimbriae and CT induced both Ag-specific Th1/Th2-type responses in $CD4^+$ T cells in mucosal effector tissues [39], while co-administration of tetanus toxoid or OVA resulted in the generation of antigen-specific Th2-type responses [30]. We still do not fully understand the exact molecular/cellular mechanisms by which nasal administration of Stx derivatives enhances Th2-type responses. However, given the promise and potency of non-toxic Stx derivatives as mucosal adjuvants, we are vigorously pursuing the elucidation of these mechanisms.

It is interesting to note that Stx1-B possessed a mucosal adjuvant activity equally as good as that of mStx1. Since Stx1-B binds to the Gb cell surface receptor, the signaling pathways through Gb3 may have immunomodulating activities. In this regard, it is well known that CT-B binds to GM1 ganglioside [40]. Further, other studies have demonstrated that GM1-mediated signaling enhances endocytosis as well as antigen presentation of APC including macrophages and DC. Further, glycosphingolipids such as GM1 have also been implicated as a delivery site for immune-enhancing signals [41]. This contention is supported by findings that rCT-B provides some mucosal adjuvant activity when given nasally [42,43]. Taken together, these findings suggest that interactions between Stx1-B and Gb3, like those between CT-B and GM1, may enhance immune responses. However, other studies including ours have reported that rCT-B does not appear to be as effective as the native form (e.g., holotoxin) in enhancing antigen-specific immune responses [30,44]. Thus, in general higher doses of rCT-B than of the native form have been used to demonstrate mucosal adjuvant activity [42,43]. Taken together, these previous studies along together with our results suggest that the immunomodulating activities induced by Stx1-B/Gb3 interactions may be much higher than those induced by CT-B/GM1 interactions. Studies are underway to elucidate this interesting possibility.

The results of this study have also shown that the administration of mStx1 harboring two mutations at the active site of RNA *N*-glycosidase activity fostered some adjuvant activity. High levels of serum Ag-specific IgG Ab and mucosal IgA Ab responses were induced in mice nasally immunized with OVA and mStx1. In order to develop a safe mucosal immunoenhancer, one that is non-toxic but retains adjuvanticity, a number of non-toxic mutant derivatives of CT or LT have been developed and characterized [25,30,32,45]. Early studies have suggested that ADP-ribosyltransferase activity is essential for the adjuvanticity of both LT and CT [44]. However, single amino acid-substituted mutants of CT S61F, E112K [25,30], P106S, S63K [46] and LT R7K [47], S63K [48], A72R [49] and R192G [50], which lack ADP-ribosyltransferase activity, were shown nevertheless to retain their adjuvanticity. Our results here support the latter group of findings by suggesting that toxic and adjuvant activities are separated from each other in the enzyme activity cleft of the bacterial toxins, including Stxs, CT and LT.

In the past, several different non-toxic mutant derivatives of CT or LT have been developed and characterized for their adjuvanticity [25,30,32,45]. In our separate study, it was shown that mutant CT (mCT of E112K and S61F) possessed adjuvanticity for supporting Th2 mediated IgA antibody responses [25,30]. Since these different forms of mutant CT and LT retain their adjuvanticity, we could consider to use one of these different forms of mutant CT and LT as a gold standard for mStx1 and Stx1-B. However, we have to realize the fact that Stx1 is completely different toxin molecule when compared with CT and LT in terms of biological activity and primary structure. For example, Stx has RNA *N*-glycosidase activity and cleaves a specific *N*-glycosidic bond in the 28S rRNA, thereby inhibiting the peptide chain elongation step of protein synthesis and ultimately causing cell death [51]. On the other hand, CT catalyzes ADP ribosylation of the G protein, Gsα which activates adenylate cyclase, resulting in elevation of intracellular cAMP levels, which causes secretion of water and chloride ions from epithelial cells into the small intestine [40]. The eukaryotic cell surface receptors for the members of Stx and CT families are globotriaosylceramide and GM1 ganglioside, respectively [40,51]. Thus, it might not be appropriate to compare Stx1 type and CT (or LT) type toxin-based adjuvants.

It has been suggested that the dose of adjuvant used for immunization can influence the adjuvant activity [52]. Thus, a simple notion is that adjuvanticity of manipulated toxin-based molecules can be demonstrated for every toxin-based adjuvant by increasing dose used for immunization. In the case of Stx1 derivatives, when a dose of 0.5 μg was employed for both Stx1-B and mStx1, the levels of serum Ag-specific Ab responses in Stx1-B-treated mice were lower than those seen in mStx1-treated groups (data not shown). However, the titer of Ag-specific Ab responses in Stx1-B-treated group was elevated in accordance to the increase of dose used (e.g., 5 μg) (data not shown). The adjuvanticity of mStx1 reached to plateau level at the dose of more than 0.5 μg (data not shown). Our data at least suggested that the dose effect of adjuvanticity was most obvious for Stx1-B when compared with that of mStx1. Inas much as a major purpose of our present study was to elucidate mucosal adjuvant activity of Stx1 derivatives including Stx1-B and mStx1, the optimal dose for these two molecules (5 and 0.5 μg, respectively) were determined and then employed for this study. Based on the present finding, our next goal is to determine the exact molecular mechanisms involved in mStx1 and Stx1-B mediated adjuvant activities. To investigate the differences between the mechanisms of adjuvanticity of mStx1 and Stx1-B, one possible

and interesting experiment would be to compare the induction and regulation of Th2 associated signaling events including GATA-3, c-maf or SLAT by mStx1 or Stx1-B since our result suggested that both Stx1-based adjuvants resulted in the induction of Th2 cell associated Ag-specific IgG1 and IgA responses (Figs. 1 and 3). To this end it has been shown that these signaling molecules are specifically associated with the Th2 cell differentiation [53,54].

In summary, this study has shown that nasal immunization with protein Ag plus mStx1 or Stx1-B as mucosal adjuvant elicits Ag-specific $CD4^+$ Th2 cells in both mucosal and systemic tissues, and these cells in turn induce antigen-specific IgA and IgG Ab responses in the mucosal and systemic compartments, respectively. Non-toxic Stx derivatives could then be considered as new and promising candidates for mucosal adjuvants.

Acknowledgements

We appreciate the constructive comments regarding this work made by members of the Division of Immunology and Medical Zoology at Niigata University Graduate School of Medical and Dental Sciences and members of the Department of Mucosal Immunology, Research Institute for Microbial Diseases, Osaka University.

This study was supported by a grant from the Ministry of Health, Labor and Welfare, the Ministry of Education, Science, Sports and Culture, CREST, JST in Japan, and Special Coodination Funds for Promoting Science and Technology from the Ministry of Education, Culture, Sports, Science and Technology, the Japanese Government.. M.O. is supported by the Japanese Human Health Science Foundation.

All experiments described herein were approved by the appropriate local authorities. All procedures were in agreement with NIH guidelines for the handling of laboratory animals.

References

[1] Mestecky J, McGhee JR. Immunoglobulin A (IgA): molecular and cellular interactions involved in IgA biosynthesis and immune response. Adv Immunol 1987;40:153–245.

[2] Clements JD, Hartzog NM, Lyon FL. Adjuvant activity of *Escherichia coli* heat-labile enterotoxin and effect on the induction of oral tolerance in mice to unrelated protein antigens. Vaccine 1988;6(3):269–77.

[3] Elson CO, Ealding W. Generalized systemic and mucosal immunity in mice after mucosal stimulation with cholera toxin. J Immunol 1984;132(6):2736–41.

[4] Xu-Amano J, Kiyono H, Jackson RJ, et al. Helper T cell subsets for immunoglobulin A responses: oral immunization with tetanus toxoid and cholera toxin as adjuvant selectively induces Th2 cells in mucosa associated tissues. J Exp Med 1993;178(4):1309–20.

[5] Katz JM, Lu X, Young SA, Galphin JC. Adjuvant activity of the heat-labile enterotoxin from enterotoxigenic *Escherichia coli* for oral administration of inactivated influenza virus vaccine. J Infect Dis 1997;175(2):352–63.

[6] Marinaro M, Staats HF, Hiroi T, et al. Mucosal adjuvant effect of cholera toxin in mice results from induction of T helper 2 (Th2) cells and IL-4. J Immunol 1995;155(10):4621–9.

[7] Takahashi I, Marinaro M, Kiyono H, et al. Mechanisms for mucosal immunogenicity and adjuvancy of *Escherichia coli* labile enterotoxin. J Infect Dis 1996;173(3):627–35.

[8] Birnabaum S, Pinto M. Local and systemic opsonic adherent. Z Immunitatsforsch Exp Klin Immunol 1976;151(1–2):69–77.

[9] Roberts M, Bacon A, Rappuoli R, et al. A mutant pertussis toxin molecule that lacks ADP-ribosyltransferase activity, PT-9K/129G, is an effective mucosal adjuvant for intranasally delivered proteins. Infect Immun 1995;63(6):2100–8.

[10] Ryan M, McCarthy L, Rappuoli R, Mahon BP, Mills KH. Pertussis toxin potentiates Th1 and Th2 responses to co-injected antigen: adjuvant action is associated with enhanced regulatory cytokine production and expression of the co-stimulatory molecules B7- 1, B7-2 and CD28. Int Immunol 1998;10(5):651–62.

[11] Mrsny RJ, Daugherty AL, Fryling CM, FitzGerald DJ. Mucosal administration of a chimera composed of Pseudomonas exotoxin and the gp120 V3 loop sequence of HIV-1 induces both salivary and serum antibody responses. Vaccine 1999;17(11–12):1425–33.

[12] Suckow MA, Keren DF, Brown JE, Keusch GT. Stimulation of gastrointestinal antibody to Shiga toxin by orogastric immunization in mice. Immunol Cell Biol 1994;72(1):69–74.

[13] Donohue-Rolfe A, Acheson DW, Keusch GT. Shiga toxin: purification, structure, and function. Rev Infect Dis 1991;13(Suppl 4):S293–7.

[14] Endo Y, Tsurigi K, Yutsudo T, Takeda Y, Ogasawara T, Igarashi K. Site of action of a Vero toxin (VT2) from *Escherichia coli* O157: H7 and of Shiga toxin on eukaryotic ribosomes RNA *N*-glycosidase activity of the toxins. Eur J Biochem 1988;171:45–50.

[15] Saxena SK, O'Brien AD, Ackerman EJ. Shiga toxin, Shiga-like toxin II variant, and ricin are all single-site RNA *N*-glycosidases of 28 S RNA when microinjected into *Xenopus oocytes*. J Biol Chem 1989;264(1):596–601.

[16] Samuel JE, Perera LP, Ward S, O'Brien AD, Ginsburg V, Krivan HC. Comparison of the glycolipid receptor specificities of Shiga-like toxin type II and Shiga-like toxin type II variants. Infect Immun 1990;58(3):611–8.

[17] Stockbine N, Marques L, Newland J, Smith H, Holmes R, O'Brien A. Two toxin-converting phages from *Escherichia coli* O157: H7 strain 933 encode antigenically distinct toxins with similar biologic activities. Infect Immun 1986;53:135–40.

[18] Ohmura M, Yamasaki S, Kurazono H, Kashiwagi K, Igarashi K, Takeda Y. Characterization of non-toxic mutant toxins of Vero toxin 1 that were constructed by replacing amino acids in the A subunit. Microb Pathog 1993;15(3):169–76.

[19] Ito H, Yutsudo T, Hirayama T, Takeda Y. Isolation and some properties of A and B subunits of Vero toxin 2 and in vitro formation of hybrid toxins between subunits of Vero toxin 1 and Vero toxin 2 from *Escherichia coli* O157:H7. Microb Pathog 1988;5(3):189–95.

[20] Byun Y, Ohmura M, Fujihashi K, et al. Nasal immunization with *E. coli* verotoxin 1 (VT1)-B subunit and a nontoxic mutant of cholera toxin elicits serum neutralizing antibodies. Vaccine 2001;19(15–16):2061–70.

[21] Larsson R, Rocksen D, Lilliehook B, Jonsson A, Bucht A. Dose-dependent activation of lymphocytes in endotoxin-induced airway inflammation. Infect Immun 2000;68(12):6962–9.

[22] Ultrich JT, Cantrell JL, Gustafson GL, Rudbach JA, Hiernant JR. The adjuvant activity of monophsphoryl lipid A. Boca Raton, FL: CRC Press; 1991. p. 133–43.

[23] Yamamoto M, Briles DE, Yamamoto S, Ohmura M, Kiyono H, McGhee JR. A nontoxic adjuvant for mucosal immunity to pneumococcal surface protein A. J Immunol 1998;161(8):4115–21.

[24] VanCott JL, Staats HF, Pascual DW, et al. Regulation of mucosal and systemic antibody responses by T helper cell subsets, macrophages, and derived cytokines following oral immunization with live recombinant *Salmonella*. J Immunol 1996;156(4):1504–14.

[25] Yamamoto S, Takeda Y, Yamamoto M, et al. Mutants in the ADP-ribosyltransferase cleft of cholera toxin lack diarrheagenicity but retain adjuvanticity. J Exp Med 1997;185(7):1203–10.
[26] Swiggard W, Noncas MD, Witmer-Pack MD, Steinman RM. Enrichment of dendritic cells by plastic adherence and EA rosetting. In: Coligan JE, editor. Current Protocols in Immunology. Wiley, NY; 1991. p. 3.7.1–11.
[27] Macatonia SE, Knight SC, Edwards AJ, Griffiths S, Fryer P. Localization of antigen on lymph node dendritic cells after exposure to the contact sensitizer fluorescein isothiocyanate. Functional and morphological studies. J Exp Med 1987;166(6):1654–67.
[28] Austin PR, Hovde CJ. Purification of recombinant shiga-like toxin type I B subunit. Protein Exp Purif 1995;6(6):771–9.
[29] Kojio S, Zhang H, Ohmura M, Gondaira F, Kobayashi N, Yamamoto T. Caspase-3 activation and apoptosis induction coupled with the retrograde transport of shiga toxin: inhibition by brefeldin A. FEMS Immunol Med Microbiol 2000;29(4):275–81.
[30] Yamamoto S, Kiyono H, Yamamoto M, et al. A nontoxic mutant of cholera toxin elicits Th2-type responses for enhanced mucosal immunity. Proc Natl Acad Sci USA 1997;94(10):5267–72.
[31] Yamamoto M, Kiyono H, Yamamoto S, et al. Direct effects on antigen-presenting cells and T lymphocytes explain the adjuvanticity of a nontoxic cholera toxin mutant. J Immunol 1999;162(12):7015–21.
[32] Cong Y, Weaver CT, Elson CO. The mucosal adjuvanticity of cholera toxin involves enhancement of costimulatory activity by selective up-regulation of B7.2 expression. J Immunol 1997;159(11):5301–8.
[33] Jones HP, Hodge LM, Fujihashi K, Kiyono H, McGhee JR, Simecka JW. The pulmonary environment promotes Th2 cell responses after nasal-pulmonary immunization with antigen alone, but Th1 responses are induced during instances of intense immune stimulation. J Immunol 2001;167(8):4518–26.
[34] Wilson AD, Bailey M, Williams NA, Stokes CR. The in vitro production of cytokines by mucosal lymphocytes immunized by oral administration of keyhole limpet hemocyanin using cholera toxin as an adjuvant. Eur J Immunol 1991;21(10):2333–9.
[35] Iwasaki A, Kelsall BL. Freshly isolated Peyer's patch, but not spleen, dendritic cells produce interleukin 10 and induce the differentiation of T helper type 2 cells. J Exp Med 1999;190(2):229–39.
[36] Gagliardi MC, Sallusto F, Marinaro M, Langenkamp A, Lanzavecchia A MT. Cholera toxin induces maturation of human dendritic cells and licences them for Th2 priming. Eur J Immunol 2000;30(8):2394–403.
[37] de Jong EC, Vieira PL, Kalinski P, et al. Microbial compounds selectively induce Th1 cell-promoting or Th2 cell-promoting dendritic cells in vitro with diverse th cell-polarizing signals. J Immunol 2002;168(4):1704–9.
[38] Ausiello CM, Fedele G, Urbani F, Lande R, Di Carlo B, Cassone A. Native and genetically inactivated pertussis toxins induce human dendritic cell maturation and synergize with lipopolysaccharide in promoting T helper type 1 responses. J Infect Dis 2002;186(3):351–60.
[39] Yanagita M, Hiroi T, Kitagaki N, et al. Nasopharyngeal-associated lymphoreticular tissue (NALT) immunity: fimbriae-specific Th1 and Th2 cell-regulated IgA responses for the inhibition of bacterial attachment to epithelial cells and subsequent inflammatory cytokine production. J Immunol 1999;162(6):3559–65.
[40] Spangler BD. Structure and function of cholera toxin and the related *Escherichia coli* heat-labile enterotoxin. Microbiol Rev 1992;56(4):622–47.
[41] Simons K, Ikonen E. Functional rafts in cell membranes. Nature 1997;387(6633):569–72.
[42] Isaka M, Yasuda Y, Kozuka S, et al. Induction of systemic and mucosal antibody responses in mice immunized intranasally with aluminium-non-adsorbed diphtheria toxoid together with recombinant cholera toxin B subunit as an adjuvant. Vaccine 1999;18(7–8):743–51.
[43] Tochikubo K, Isaka M, Yasuda Y, et al. Recombinant cholera toxin B subunit acts as an adjuvant for the mucosal and systemic responses of mice to mucosally co-administered bovine serum albumin. Vaccine 1998;16(2–3):150–5.
[44] Lycke N, Tsuji T, Holmgren J. The adjuvant effect of *Vibrio cholerae* and *Escherichia coli* heat-labile enterotoxins is linked to their ADP-ribosyltransferase activity. Eur J Immunol 1992;22(9):2277–81.
[45] Elson CO, Holland SP, Dertzbaugh MT, Cuff CF, Anderson AO. Morphologic and functional alterations of mucosal T cells by cholera toxin and its B subunit. J Immunol 1995;154(3):1032–40.
[46] Douce G, Fontana M, Pizza M, Rappuoli R, Dougan G. Intranasal immunogenicity and adjuvanticity of site-directed mutant derivatives of cholera toxin. Infect Immun 1997;65(7):2821–8.
[47] Douce G, Turcotte C, Cropley I, et al. Mutants of *Escherichia coli* heat-labile toxin lacking ADP-ribosyltransferase activity act as nontoxic, mucosal adjuvants. Proc Natl Acad Sci USA 1995;92(5):1644–8.
[48] Di Tommaso A, Saletti G, Pizza M, et al. Induction of antigen-specific antibodies in vaginal secretions by using a nontoxic mutant of heat-labile enterotoxin as a mucosal adjuvant. Infect Immun 1996;64(3):974–9.
[49] Giuliani MM, Del Giudice G, Giannelli V, et al. Mucosal adjuvanticity and immunogenicity of LTR72, a novel mutant of *Escherichia coli* heat-labile enterotoxin with partial knockout of ADP- ribosyltransferase activity. J Exp Med 1998;187(7):1123–32.
[50] Dickinson BL, Clements JD. Dissociation of *Escherichia coli* heat-labile enterotoxin adjuvanticity from ADP-ribosyltransferase activity. Infect Immun 1995;63(5):1617–23.
[51] Paton JC, Paton AW. Pathogenesis and diagnosis of Shiga toxin-producing *Escherichia coli* infections. Clin Microbiol Rev 1998;11(3):450–79.
[52] Rappuoli R, Pizza M, Douce G, Dougan G. Structure and mucosal adjuvanticity of cholera and *Escherichia coli* heat-labile enterotoxins. Immunol Today 1999;20(11):493–500.
[53] Kuo CT, Leiden JM. Transcriptional regulation of T lymphocyte development and function. Annu Rev Immunol 1999;17:149–87.
[54] Madrenas J. A SLAT in the Th2 signalosome. Immunity 2003;18(4):459–61.

Available online at www.sciencedirect.com

SCIENCE DIRECT

Clinical Immunology 113 (2004) 326–339

CLINICAL IMMUNOLOGY

www.elsevier.com/locate/yclim

Biological role of Ep-CAM in the physical interaction between epithelial cells and lymphocytes in intestinal epithelium

Tomonori Nochi[a,b,c], Yoshikazu Yuki[a,c], Kazutaka Terahara[a,c], Ayako Hino[a,c], Jun Kunisawa[a], Mi-Na Kweon[a,d], Takahiro Yamaguchi[b], Hiroshi Kiyono[a,c,*]

[a]*Division of Mucosal Immunology, Department of Microbiology and Immunology, The Institute of Medical Science, The University of Tokyo, Tokyo 108-8639, Japan*

[b]*Laboratory of Functional Morphology, Division of Life Science, Department of Animal Biology, The Graduate School of Agricultural Science, Tohoku University, 981-8555, Japan*

[c]*CREST, Japan Science and Technology, 332-0012, Japan*

[d]*Division of Mucosal Immunology, International Vaccine Institute, 151-600, South Korea*

Received 13 August 2004; accepted with revision 24 August 2004
Available online 29 September 2004

Abstract

The mucosal epithelium including intestinal epithelial cells (IECs) and intraepithelial lymphocytes (IELs) provide a first line of defense in the gastrointestinal tract. However, limited information is currently available concerning the nature of the physical interaction molecule that interconnects IECs and IELs. Among the several monoclonal antibodies (mAbs) generated by immunizing porcine IECs, mAb (5-15-1) was shown to strongly react with IELs in addition to IECs. MALDI-TOF-MS and tandem MS analysis suggested that the antigen belongs to a family of human homophilic epithelial cell adhesion molecule (Ep-CAM). The amino acid sequence of porcine Ep-CAM showed 82.8%, 78.1%, and 76.8% homology compared to human, mouse, and rat Ep-CAM. Moreover, 5-15-1 specifically reacted with transfectant of porcine Ep-CAM. These data suggest that the Ep-CAM may act as a physical homophilic interaction molecule between IELs and IECs at the mucosal epithelium for providing immunological barrier as a first line of defense against mucosal infection.

Keywords: Mucosa; Epithelial cell; Intraepithelial lymphocyte; Adhesion molecule; Cell surface molecule; Cell trafficking

Introduction

Intestinal epithelial cells (IECs) originate from and are maintained by a small number of pluripotent stem cells in crypts and have a life span of 2–4 days [1]. IECs have long been known to absorb nutrients into the circulation. More recently, IECs have also been found to act as an important immunological barrier against pathogens or nonself antigens and thus to comprise a major compartment of the mucosal immune system. They are equipped with mucus and antibacterial enzymes (e.g., lysozyme), which act as innate barriers, and secretory IgA (S-IgA) and T cell-mediated immunity, which serve as acquired barriers [2]. To preserve the integrity of the first line of defense against pathogens, IECs are welded together by a number of adhesion mechanisms. For example, tight junctions consisting of occludin [3] and the family of claudin [4,5] have been shown to play a central role in sealing the intracellular space between epithelial cells [6–8]. E-cadherin, another adhesion molecule expressed by epithelial cells, homophilically regulates Ca^{2+}-dependent interactions at the site of the tight junction [9]. The extracellular domain of E-cadherin is composed of five repeats and contain Ca^{2+} binding motifs [10]. Cadherin forms tight complexes with three cytoplasmic proteins, α-, β-, and γ-catenin, linked to the actin cytoskeleton [11]. This unique cell-to-cell adhesion system

* Corresponding author. Division of Mucosal Immunology, Department of Microbiology and Immunology, The Institute of Medical Science, The University of Tokyo, 4-6-1 Shirokanedai, Minato-ku, Tokyo 108-8639, Japan. Fax: +81 3 5449 5411.

E-mail address: kiyono@ims.u-tokyo.ac.jp (H. Kiyono).

1521-6616/$ - see front matter © 2004 Elsevier Inc. All rights reserved.
doi:10.1016/j.clim.2004.08.013

of IECs helps maintain a physiologically normal intestinal epithelium by serving as both a physical and immunological barrier against the invasion of undesirable foreign substances. On the other hand, under the condition of sever mucosal inflammation (e.g., inflammatory bowel diseases), the expression of these epithelial intercellular junction proteins was down-regulated by transmigrating neutrophils from intestinal lamina propria to lumen [12]. Thus, a group of these adhesion molecules associating with the formation of mucosal epithelium is directly influenced by the process of development of inflammation.

Most intraepithelial lymphocytes (IELs), which are present in large numbers in the intestinal epithelium, are $CD3^+$ T cells and are expressed by heterodimer chains of either αβ or γδ T cell receptors (TCR). In mice, IEL expression is almost evenly divided between αβ and γδ TCR [13]. Although their exact immunological functions remain unknown, these IELs have been shown to be involved in both the innate and acquired phases of mucosal immunity [14]. IELs bearing γδTCR (γδIELs) possess several features that distinguish them from αβIELs. For example, γδIELs exclusively express the CD8αα homodimer or doubly negative for CD4 and CD8 and are thought to be developed extrathymically [15]. In addition, γδIELs are absent in mice lacking a common cytokine receptor γ chain, which is a subunit of the receptor for IL-2, IL-4, IL-7, IL-9, and IL-15 [16]. The unique immunological and microbiological environment of the intestinal epithelium perhaps contributes to the creation of subsets of IEL-associated T cells distinct from the thymus-originated T cells located in the peripheral lymph nodes.

A number of recent findings suggest that a reciprocal dependency exists between IECs and IELs and that it is under the regulation of a group of intestinal epithelium-associated cytokines, including IL-7, IL-15, and SCF [17–19]. IECs are capable of producing IL-7 and IL-15, important cytokines for the stimulation and development of γδIELs expressing the corresponding receptor [20–22], while γδIELs have been shown to produce SCF, which stimulates the growth of IECs [19]. These results clearly indicate that an array of interactions between cytokines and their corresponding receptors play an important role in the formation and maintenance of the monolayer of the mucosal epithelium. Further, it has been suggested that IECs and IELs form mucosal intranet and provide a first line of defense at mucosal epithelium [2]. IEC-derived IL-15 has been shown to be a key regulatory molecule for the generation of IELs including γδT cells-mediated immunological barrier function [23]. On the other hand, overproduction of IL-15 at the mucosal epithelium resulted in the development of intestinal inflammation [24]. A similar aberrant condition was also triggered by the overproduction of IL-7 at mucosal epithelium [25]. These findings further emphasize the importance of mucosal intranet operated by IECs and IELs for the control of inflammation and infection. However, minimal information is currently available regarding the cellular and molecular mechanisms underlying the physical cell-to-cell interactions between IECs and IELs via the cell surface adhesion molecule. To address this gap in the data, we have sought in this study to elucidate the molecular basis for the physical cell-to-cell interactions between IECs and IELs by generating monoclonal antibodies (mAbs) to react with the cell surface of both IECs and IELs.

Materials and methods

Animal

Female Balb/c mice (6 weeks old) were purchased from CREA (Tokyo, Japan) and maintained in the experimental animal facility at the Institute of Medical Science, the University of Tokyo. The tissues of male and female three-way cross-bred pigs were purchased from Tokyo Shibaura Zouki (Tokyo, Japan). All of the tissues were obtained from 6-month-old pigs. In some cases, the tissues were kindly provided from Chugai Research Institute for Medical Science (Nagano, Japan).

Isolation of porcine IECs from the small intestine

IECs were physically and enzymatically isolated from porcine small intestines. First, the small intestines were washed with cold PBS and then torn into muscle layers. The tissues were then cut into small fragments of 1–2 cm and digested with 1 mg/ml collagenase (Wako, Osaka, Japan) and 1 mg/ml hyaluronidase (Sigma, Saint Louis, MO) in PBS at 37°C for 20 min. After digestion, tissue was washed again with cold PBS and then redigested with 1 mg/ml pancreatin (Sigma) in 25 mM HEPES buffer at 37°C for 15 min. Isolated cells were washed with cold PBS and then purified using a 45% Percoll gradient (Amasham Pharmacia Biotech, Uppsala, Sweden). Following centrifugation, the upper layer of cells was collected and stained first with mouse IgG1 anti-porcine CD45 mAb (K252.1E4, Serotec Ltd., Oxford, UK) diluted 1:10 at 4°C for 30 min and then by microbead-conjugated rat anti-mouse IgG1 (Miltenyi Biotec, Bergisch Gladbach, Germany) diluted 1:5 at 4°C for 15 min to further remove contaminated leukocytes. Finally, IECs were negatively selected by auto-MACS (Miltenyi Biotec). Immunostaining with anti-cytokeratin mAb (Sigma) showed that the resulting IEC preparation was highly purified (>95%) [26].

Generation of mouse monoclonal antibodies

Purified porcine IECs were used for intraperitoneal immunization of BALB/c mice (2.0×10^6 cells/mouse). After 1 week, the mice received a booster intravenous injection of porcine IECs (1.0×10^6 cells/mouse). Four days after the booster, the mice were sacrificed so that splenic mononuclear cells could be harvested. Splenocytes

were fused with Sp2/0-Ag14 myeloma cells (ATCC, CRL-1581) in the presence of 50% (w/v) polyethylene glycol 1500 (Roche, Mannheim, Germany). Supernatants from the resulting hybridomas were screened with isolated cells from the small intestine by flow cytometry analysis. The isotype of the porcine IEC-reactive hybridoma was determined using a mouse monoclonal antibody-isotyping kit (Amersham Pharmacia Biotech). The mAbs, produced in the ascitic fluids of BALB/c mice by priming with pristane (Wako), were purified using Protein G sepharose (Amersham Pharmacia Biotech). Purified mAbs were biotinylated with EZ-Link Sulfo-NHS-LC-biotin (PIERCE, Rockford, IL). Among 10 mAbs generated, one clone of mAb (5-15-1: mouse IgG2b) was selected for the present study due to its specific and strong reactivity with the porcine intestinal epithelium. An optimal concentration of mAb (5-15-1) was determined for the different assay system used in this study, and those doses are indicated for the respective protocol or figure legend.

Immunohistochemistry

The porcine tissues were fixed in 4% paraformaldehyde (Wako), incubated overnight at 4°C, and then washed with 8% and 16% (w/v) sucrose solutions before being incubated overnight again at 4°C. The tissues were then embedded in Tissue-Tek OCT compound (SAKURA Finetechnical Company, Ltd., Tokyo, Japan). Tissue sections (5 μm) were incubated with 1.5% (v/v) normal goat serum (Vector, Burlingame, CA) for 20 min at room temperature (RT). They were then incubated overnight at 4°C with 10 μg/ml purified mAb (5-15-1, mouse IgG2b) and/or anti-porcine CD45 mAb (mouse IgG1, Serotec, Ltd.) diluted 1:10 or an isotype control (mouse IgG1 and/or mouse IgG2b, BD PharMingen, San Jose, CA). For single staining, they were incubated with FITC-conjugated goat anti-mouse IgG (IMMUNOTECH, Marseille, France) diluted 1:200 for 1 h at RT, and for double staining with FITC-conjugated anti-mouse IgG2b (Santa Cruz Biotechnology, Santa Cruz, CA) diluted 1:100 and rhodamine-conjugated anti-mouse IgG1 (Santa Cruz Biotechnology) diluted 1:100. Finally, the sections were counterstained with 1 μg/ml propidium iodate (Sigma) or 200 ng/ml DAPI (Sigma) for 30 min at RT and analyzed using a confocal laser scanning microscope (TCS SP2, Leica, Wetzlar, Germany).

Immunoprecipitation and Western blot analysis

The lysate of several tissues were washed with cold PBS and lysed in lysis buffer [50 mM Tris–HCl (pH 7.5), 150 mM NaCl, 0.5% Triton X-100, and a protease inhibitor cocktail (Roche)]. After 1 h of incubation on ice followed by centrifugation, the lysate (5 mg/ml, 1 ml) was precleared with 40 μl protein G Sepharose (1:1 in PBS, Amersham Pharmacia Biotech) at 4°C for 1 h. After centrifugation, the lysate was incubated with mAb (5-15-1, 10 μg/ml) or an isotype control (mouse IgG2b, BD PharMingen) for 1 h at 4°C, before the addition of 40 μl Protein G Sepharose (1:1 in PBS) and incubation for 1 h at 4°C. Immune complexes were washed five times with cold PBS containing a protease inhibitor cocktail and eluted in Laemmli sample buffer with or without 2-ME. They were then subjected to an SDS-PAGE using a 12.5% polyacrylamide gel (Daiichi Pure Chemical, Tokyo, Japan) before being transferred to a polyvinylidene difluoride (PVDF) membrane (MILLIPORE, Billerica, MA) using a semidry transblot system (ATTO Instruments, Tokyo, Japan). The membranes were blocked in 1% BSA, 0.2% Tween-20/PBS overnight at 4°C, and incubated with biotinylated mAb (5-15-1, 10 μg/ml) at RT for 1 h and then with ABC-AP complex (Vector) at RT for 1 h. Finally, the reaction was detected with an Alkaline phosphatase-conjugated substrate kit (Bio-Rad, Hercules, CA). Carbohydrates were also stained with G.P. Sensor (HONEN, Yokohama, Japan) in accordance with the manufacturer's instructions.

Isolation of IELs, splenocytes, and PBMCs for flow cytometric analysis

Lymphocytes were isolated from small intestinal epithelium and spleen, as described previously with some modifications [26]. Briefly, in the case of IELs, the small intestinal epithelium was prepared and then stirred at 37°C in RPMI-1640 (Sigma) containing 1 mM EDTA for 20 min. Lymphocytes from the small intestinal epithelium and spleen were separated on a Percoll density gradient (Amersham Pharmacia Biotech). The cells layered between the 40% and 75% fractions were collected as IELs and splenocytes. PBMCs were separated on NycoPrep (AXIS-SHIELD PoC AS, Oslo, Norway) after blood was mixed with two volumes of PBS. IECs, IELs, splenocytes, and PBMCs were incubated with 1 μg/ml porcine IgG (Sigma) at 4°C for 20 min and then stained with 10 μg/ml purified mAb (5-15-1) or an isotype control (mouse IgG2b, BD PharMingen) at 4°C for 30 min, before being subjected to an FITC-conjugated anti-mouse IgG (IMMUNOTECH) and 10 μl/test VIAPROBE (BD Pharmingen) for 30 min at 4°C. Finally, the cells were analyzed by flow cytometry using FACSCalibur (Becton Dickinson, Franklin Lakes, NJ).

Purification and analysis of antigen by MALDI-TOF-MS and Tandem MS after triptic digestion

The antigen of mAb (5-15-1) was purified from the lysate of the small intestine by affinity chromatography using an Affi-Gel Hz Immunoaffinity Kit (Bio-Rad). Purified antigen was analyzed by SDS-PAGE with 12.5% polyacrylamide gel and stained by GelCode Blue Stain Reagent (PIERCE). The responding protein was digested with trypsin using a method previously described [27]. The resulting peptide samples were analyzed by time-of-flight mass spectrometry (Applied Biosystems, Foster, CA) after being spotted on a

MALDI plate and co-crystallized with α-cyano-4-hydroxycinnamic acid [27]. This plate was then loaded into the QSTAR Pulser *i* (Applied Biosystems) at Hitachi Science Systems (Ibaraki, Japan).

Cloning of porcine epithelial cell adhesion molecules (Ep-CAM)

The porcine Ep-CAM gene was amplified from the mRNA of the small intestine by RT-PCR with mix primers (Sense: 5′-CDKCYAARTGYTTGGYGATG-3′ Antisense: 5′-RMCACMACSACAATRACRGC-3′) prepared based on the sequence data from humans [28], mice [29], and rats [30]. The 5′ and 3′ regions were analyzed with a GeneRacer kit (Invitrogen, Carlsbad, CA) by oligocapping and 3′RACE methods with primers prepared by the sequence data obtained from the internal porcine Ep-CAM (5′ region: 5′-AGGTCCATCCTTTTGGAATG-3′, 5′-AGGTACCATTACACTGCTTG-3′, 3′ region: 5′-ATTACCAACTGGATCCCAAA-3′, 5′-ATGAATCCTTGTTCCA-TTCC-3′). The sequencing was performed using the ABI3700 at Hitachi Science Systems (Tokyo, Japan).

Transfection of cells

Full-length porcine Ep-CAM was amplified by RT-PCR with primers (sense:5′-ATTACTAATAGCTAGCATGGCGCCCCCCCAGGTCCT-3′, antisense: 5′-AGCACTGAATTCTTATGCATTGAGTTCCCTAT-3′, *Nhe*I, and *Eco*RI restriction enzyme site showed by underlining). It was then ligated into pIRES2-EGFP Vector (BD Biosciences Clontech, Palo Alto, CA) in front of the enhanced GFP (EGFP)-coding region at the *Nhe*I and *Eco*RI sites using the DNA Ligation Kit Ver.2 (Takara Biomedicals, Shiga, Japan) and sequenced. Because it contained the internal ribosome entry site (IRES), this plasmid (pIRES2-EGFP-pEp-CAM) was able to express both porcine Ep-CAM and EGFP. pIRES2-EGFP-pEp-CAM was transfected into COS-7 (ATCC, CRL-1651) in Opti-MEM (Invitrogen) by electrophoresis using Gene Pulser Xcell (Bio-Rad) [31]. After 48 h, the cells were stained first with 10 μg/ml mAb (5-15-1) or an isotype control (mouse IgG2b, BD PharMingen), then with CY 5-conjugated anti-mouse IgG (Jackson, West Grove, PA) diluted 1:400, and finally analyzed by flow cytometry using FACSCalibur (Becton Dickinson).

Results

mAb (5-15-1) reacted with epithelium of porcine small intestine

First, isolated porcine IECs were injected into BALB/c mice to generate mAbs capable of recognizing a unique cell surface molecule of IECs. A total of 10 mAbs were generated and tested for their reactivity using frozen sections prepared from porcine small intestine by immunohistochemical analysis. One of the mAbs, designated as mAb (5-15-1) with mouse IgG2b subclass, strongly reacted with the epithelium all the way from the villus (Fig. 1Aa) to the crypt (Fig. 1Ab) regions. Interestingly, the immunoreactivity was most strongly shown on the basolateral surface of the epithelium. An isotype control (Mouse IgG2b) did not react with the tissue sections of villus and crypt epithelium (Figs. 1Ac and d).

mAb (5-15-1) reacted with the 41–43 kDa protein of porcine small intestine when Western blot analysis was performed under nonreducing conditions

Inasmuch as 5-15-1 reacted with the epithelium of the porcine small intestine, the next logical step was to elucidate the molecular weight of the antigen recognized by 5-15-1. After immunoprecipitation of the small intestine with 5-15-1, a molecular mass of 41–43 kDa protein was detected by Western blot analysis under nonreducing conditions (Fig. 1Ba). Of course, this band was not detected in the negative control using the isotype control (mouse IgG2b) for immunoprecipitation or PBS instead of the lysate of the porcine small intestine (Fig. 1Ba). Nor was the band detected under reducing conditions (Fig. 1Bb). However, the band corresponding to the 5-15-1-specific antigen was detected by a G.P. Sensor, carbohydrate detection kit (Fig. 1Bc). These findings suggest that the surface antigen recognized by 5-15-1 belongs to a family of glycoproteins.

Immunoreactivity of mAb (5-15-1) with the other epithelial cells in mucosa-associated tissues

To further examine the immunoreactivity of 5-15-1 in several other mucosa-associated and systemic tissues, tissue sections were prepared from esophagus, stomach, duodenum, jejunum, ileum, appendix, colon, lung, spleen, and liver for immunohistological examination (Fig. 2). Among mucosa-associated epithelia, esophageal epithelial cells were stratified and flattened like skins cells and did not react with 5-15-1 (Fig. 2Aa). The lamina propria of the fundus ventriculi in the stomach is composed of fundic glands located under the epithelium and characterized by chief, parietal cells, and nebenzellen cells [32,33]. The newly developed mAb 5-15-1 reacted neither with the epithelial cells (Fig. 2Ab) nor with the chief, parietal, and nebenzellen cells in the fundic glands (Fig. 2Ac). When duodenum containing glandulae duodenales were examined, duodenum epithelial cells in the villus (Fig. 2Ad), crypt (Fig. 2Ae), and glands (Fig. 2Af) reacted with 5-15-1. The intestinal tract is composed of organized lymphoid structures known as gut-associated lymphoid tissue (GALT), an important inductive site for the mucosal immune system [2]. Therefore, sections of Peyer's patches (PPs) were examined for their reactivity with 5-15-1. Follicle-associated epithelium (FAE), one of the unique features of PPs,

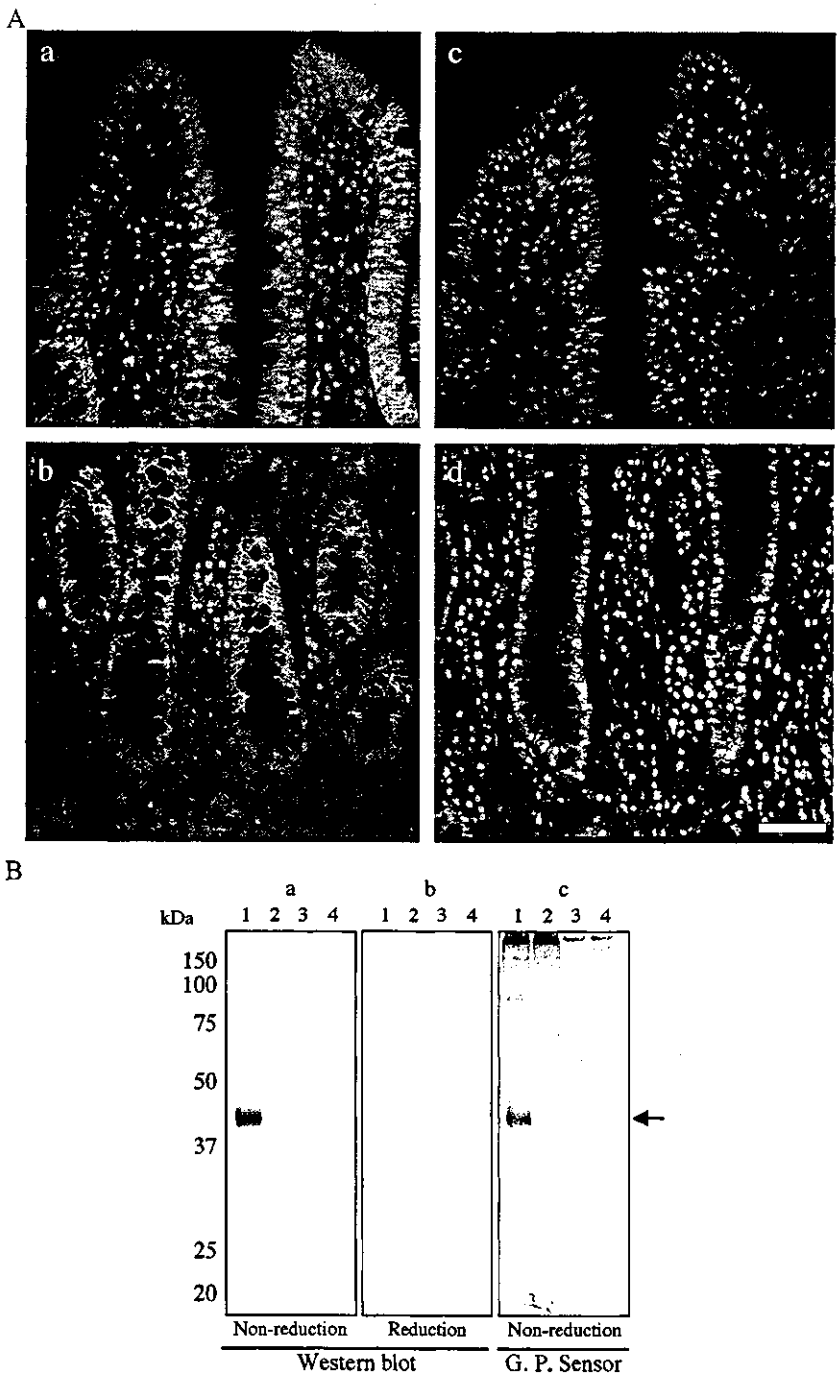

Fig. 1. Immunohistochemical and Western blot analyses of small intestine with mAb (5-15-1). Panel A shows tissue sections (5 μm) stained with the newly established mAb (5-15-1; mouse IgG2b) and with FITC-conjugated anti-mouse IgG followed by counterstaining with propidium iodate. (Aa and b) The immunoreactivity of 5-15-1; (Ac and d) the immunoreactivity of the isotype control. (Aa and c) The immunoreactivity in villus; (Ab and d) the immunoreactivity in the crypt. All of the intestinal epithelial cells (IECs) reacted with 5-15-1. Scale bar = 50 μm. Panel B shows the lysate of the small intestine (lanes 1 and 2) or the control (PBS, lanes 3 and 4), which was immunoprecipitated with 5-15-1 (lanes 1 and 3) or with an isotype control (mouse IgG2b, lanes 2 and 4) and then analyzed by Western blot. A protein measuring approximately 41–43 kDa was visible under nonreducing conditions (a) but not under reducing conditions (b). This 41–43 kDa protein was also detected under nonreducing conditions by G.P. Sensor (c).

exhibited strong immunoreactivity to 5-15-1 (Fig. 2Ag), while the leukocytes in PPs did not (Fig. 2Ah). Both the large (Fig. 2Ai) and the small (Figs. 1Aa and b) intestinal epithelium strongly reacted to 5-15-1, as did some alveolar cells and all of the epithelial cells of the bronchus in the lung (Fig. 2Aj). However, neither hepatocytes (Fig. 2Ak) nor splenocytes (Fig. 2Al) showed reactivity to 5-15-1. Looked at collectively, these results suggest that 5-15-1 specifically reacted with mucosal epithelia composed of columnar epithelial cells.

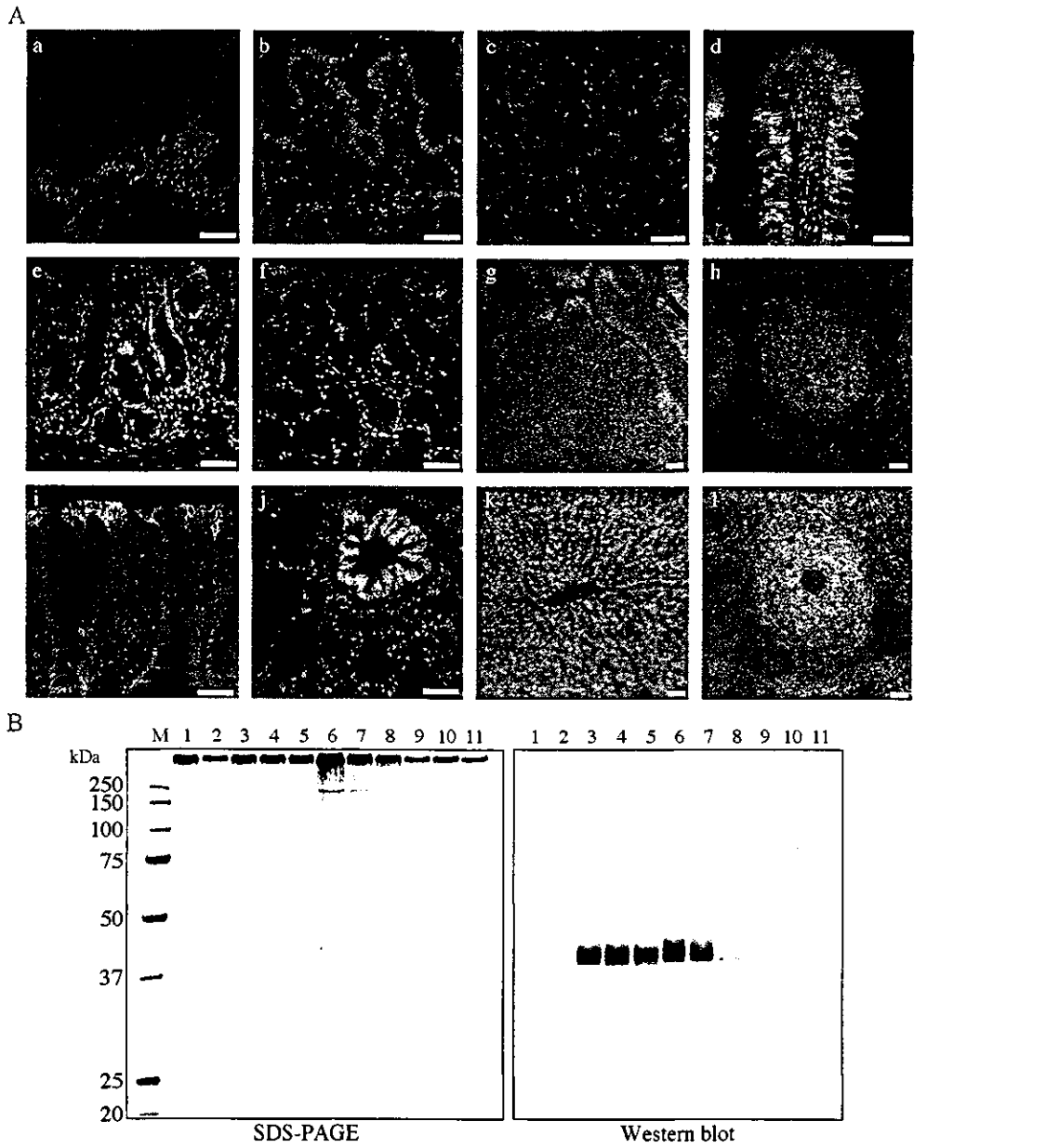

Fig. 2. Immunohistochemical and Western blot analyses of different mucosa-associated tissues with mAb (5-15-1). Panel A shows tissue sections (5 μm) stained with 5-15-1 and FITC-conjugated anti-mouse IgG followed by counterstaining with propidium iodate. Almost all of the epithelial tissues, with the exception of the esophagus and stomach, reacted with 5-15-1. (a) Esophageal epithelium, (b) stomach epithelium, (c) fundic gland in stomach, (d) epithelium in duodenum, (e) crypt in duodenum, (f) gloandulae deodenales in duodenum, (g) follicle-associated epithelium (FAE) in Peyer's patch, (h) lymphoid follicle in Peyer's patch, (i) epithelium in colon, (j) epithelium in lung, (k) hepatocyte in liver, (l) splenocyte in spleen. Scale bar = 50 μm. Panel B shows the results obtained when lysates (5 mg) of different mucosa-associated tissues were immunoprecipitated with 5-15-1 (10 μg/ml) and then analyzed by Western blot. The left panel shows the data obtained using SDS-PAGE, the right panel that obtained using Western blot. A protein with a molecular mass of 41–43 kDa was visible in the duodenum, jejunum, ileum, appendix, colon, and lung but not in the esophagus, stomach, liver, and spleen under nonreducing conditions. (1) Esophagus, (2) stomach, (3) duodenum, (4) jejunum, (5) ileum, (6) appendix, (7) colon, (8) lung, (9) liver, (10) spleen, (11) mAb alone.

Immunoprecipitation and Western blot analysis revealed the presence of the 41–43 kDa protein in all mucosa-associated tissues except the esophagus and stomach

We next used immunoprecipitation and Western blot analyses to confirm our immunohistochemical findings regarding the tissue specificity of 5-15-1 for several mucosal-associated epithelia. Lysates prepared from different mucosa-associated and systemic tissues were precipitated with 5-15-1 and then analyzed by SDS-PAGE and Western blot analyses under nonreducing conditions. The antigen corresponding to a molecular mass of 41–43 kDa was detected in the duodenum, jejunum, ileum, appendix, colon, and lung, but not in the esophagus, stomach, spleen, and liver. The results obtained by SDS-PAGE and

Western blot analyses of these different tissue extracts (Fig. 2B) confirmed the data generated by the immunohistochemical analysis (Fig. 2A). Further, the data analyzed by Western blot revealed that the expression level of the antigen was roughly equal in the duodenum, jejunum, ileum, appendix, and colon, but considerably lower in the lung (Fig. 2B).

IELs but not splenocytes and PBMCs reacted with 5-15-1

Since 5-15-1 specifically reacted with the glycoprotein antigen (41–43 kDa) associated with the intestinal epithelium, we sought to determine whether a similar protein is also expressed by neighboring IELs. Flow cytometry was used to determine the immunoreactivity to 5-15-1 of IELs and IECs isolated from porcine small intestine. Splenocytes and PBMCs isolated from the same pig served as controls. First, IELs were separated from IECs on the basis of cell size and granularity (Fig. 3a). A fraction of IELs was greater than 98% positive for CD45, while the IECs fraction did not contain any CD45-positive cells (data not shown). As expected from the findings discussed above (Fig. 1A), freshly isolated IECs were positive for 5-15-1 (Fig. 3b). Interestingly, however, IELs also reacted with 5-15-1 (Fig. 3c). When the mean fluorescence intensity of the two fractions was compared, that of IELs was weaker than that of IECs (Fig. 3f). Splenocytes (Fig. 3d) and PBMCs (Fig. 3e) did not react with 5-15-1. These findings demonstrate that the glycoprotein, which reacted with 5-15-1, was also expressed by IELs in addition to IECs in the intestinal epithelium.

MALDI-TOF-MS and tandem MS analysis of 5-15-1 reactive 41–43 kDa protein resulted in the identification of a porcine homologue of the human pan-carcinoma antigen epithelial glycoprotein (EGP), or alias epithelial adhesion molecule (Ep-CAM)

Since it was expressed by both IECs and IELs, we sought to identify the exact nature of the 41–43 kDa protein recognized by 5-15-1. The antigen was first purified from small intestine lysates using affinity chromatography with 5-15-1 and then separated out using SDS-PAGE (Fig. 4A). When the 41–43 kDa protein was analyzed by MALDI-TOF-MS analysis after tryptic digestion, several major peaks were identified (Fig. 4B). Four major peaks (asterisks) were randomly selected and further analyzed by tandem MS. The amino acid sequence of one of the peaks (arrow in Fig. 4B) was identified as IADVAYYFEK (Fig. 4C). A search of the "MASCOT" database confirmed this sequence as human pan-carcinoma antigen epithelial glycoprotein (EGP), or alias epithelial adhesion molecule (Ep-CAM). In contrast, the other three peaks were identified as actin (data not shown).

Cloning of porcine Ep-CAM

To formally prove that the antigen of 5-15-1 is a porcine homologue of human Ep-CAM, the next logical step was to clone and sequence the porcine Ep-CAM. Fig. 5 shows both the sequence including the initiation and stop codon and the predicted amino acid sequence.

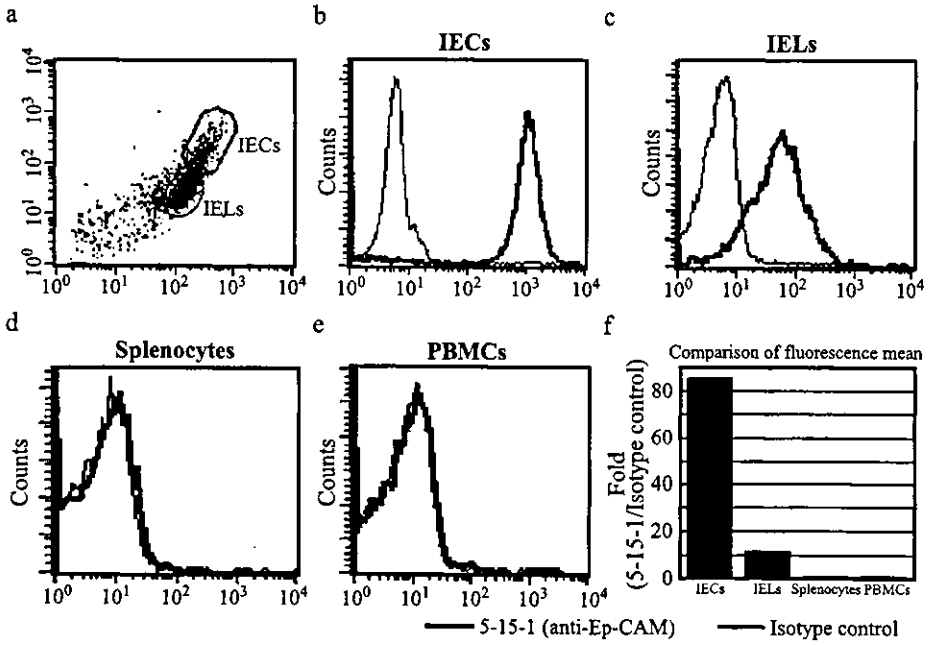

Fig. 3. Immunoreactivity of mAb (5-15-1) against IECs, IELs, splenocytes, and PBMCs. Isolated IECs, IELs, splenocytes, and PBMCs were stained with mAb (5-15-1) and FITC-conjugated anti-mouse IgG and then analyzed using flow cytometry. IECs and IELs were separated based on cell size and granularity (a). IECs (b) and IELs (c), but not splenocytes (d), and PBMCs (e) reacted with 5-15-1. The fluorescence mean intensity was also examined (f).

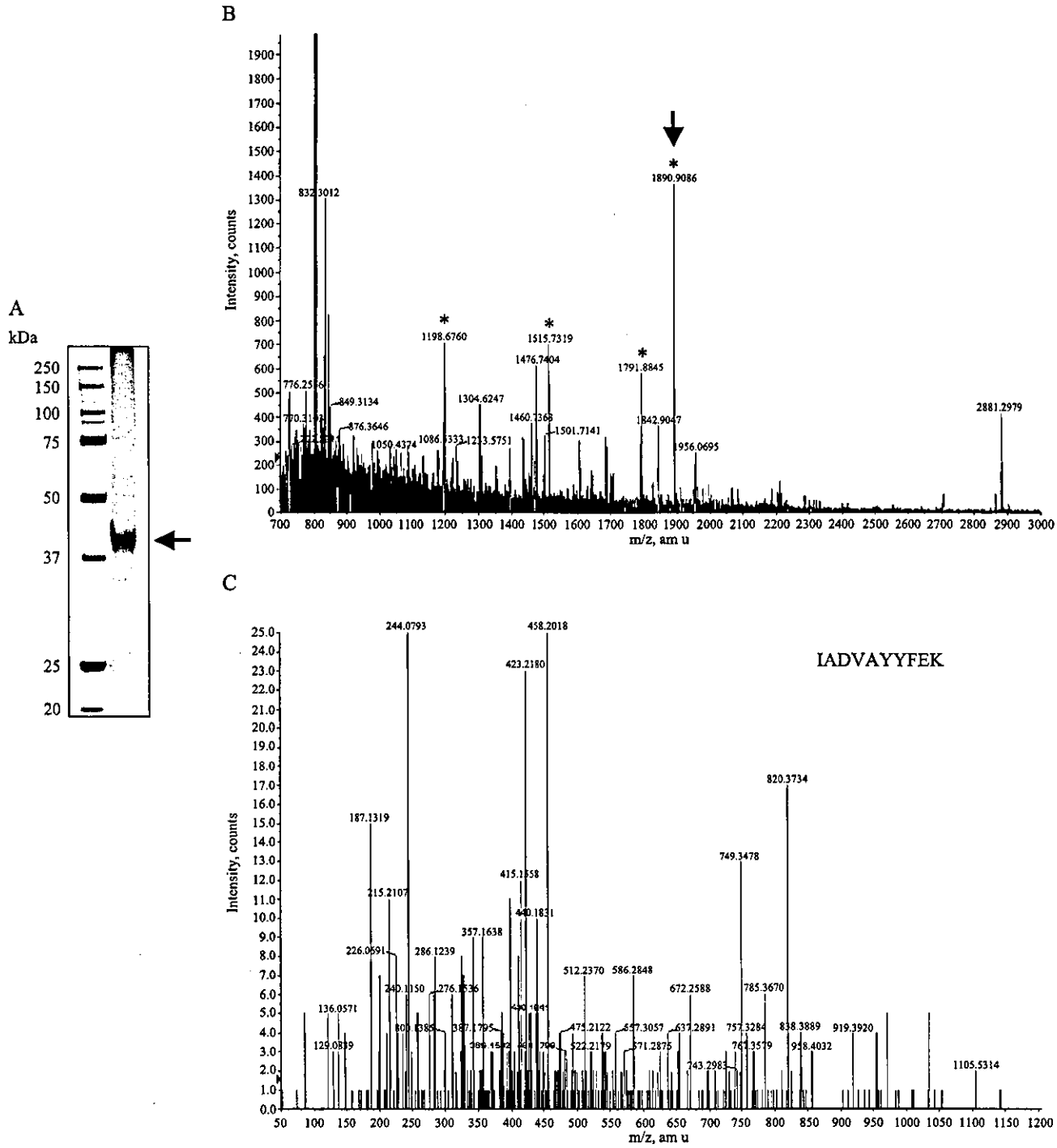

Fig. 4. Identification of the antigen purified by affinity chromatography with 5-15-1. Panel A shows the SDS-PAGE analysis of the antigen purified by affinity chromatography with 5-15-1. A protein with a molecular mass of 41–43 kDa was analyzed by MALDI-TOF-MS and tandem MS analysis. Panel B shows the MALDI-TOF-MS spectrum of the 41–43 kDa antigen digested by trypsin. Four major peaks (asterisks) were further analyzed by tandem MS. Panel C shows that the tandem MS spectrum of one of the four peaks (arrow in Panel B) was sequenced and identified as "IADVAYYFEK."

As one might expect, the cloned sequence contains tandem MS-identified "IADVAYYFEK." The sequence data were then registered with GenBank (Accession number: AB161197). The cDNA contains an open reading frame (ORF) of 945 bp and encodes for 314 amino acids. Compared with human, mouse, and rat sequences, the porcine Ep-CAM displays 82.9%, 71.3%, and 71.8% homology at the nucleotide level and 82.8%, 78.1%, and 76.8% homology at the amino acid level, respectively (Fig. 5). Porcine Ep-CAM is a type-I transmembrane protein of which the first 23 amino acids are putatively the signal sequence. A 242 amino acid, cystein-rich extracellular

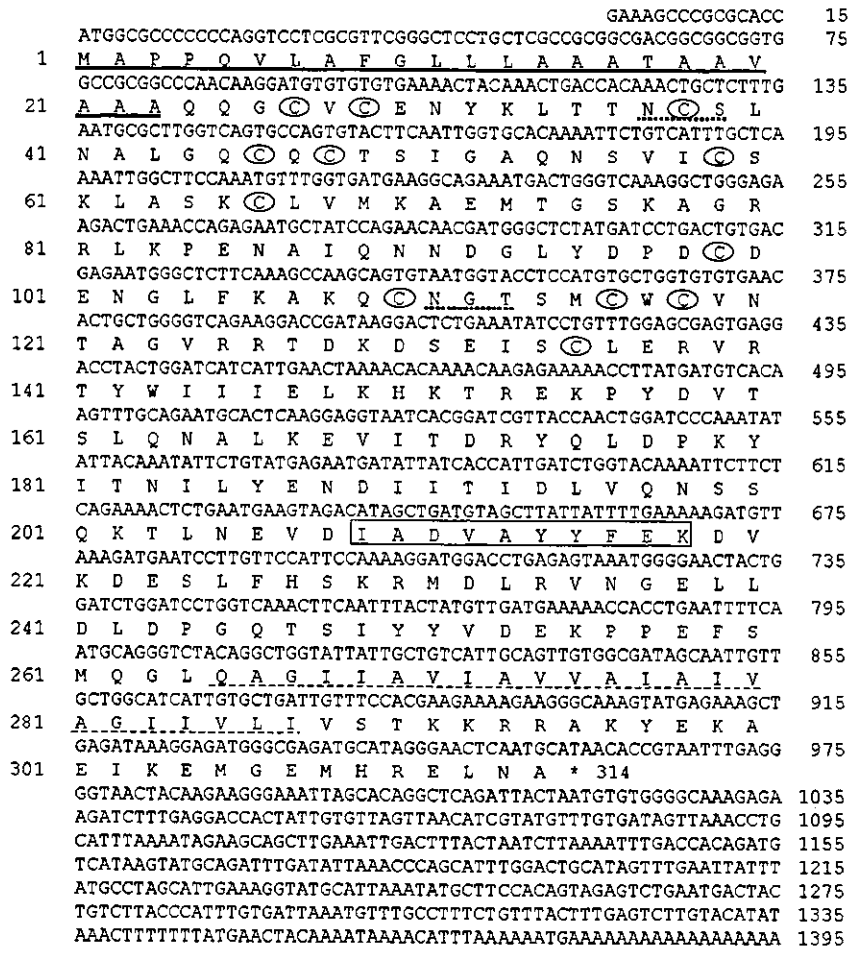

Fig. 5. DNA and amino acid sequence of porcine Ep-CAM. An open reading frame predicts a protein of 314 amino acids. A putative signal sequence (first bolded underline), 12 cysteine residues (circles), two potential N-linked glycosylation sites (bold and dotted underline), and one transmembrane domain (dotted underline) are indicated. The amino acid sequence matched that of the molecule identified by MALDI-TOF-MS and tandem MS analyses was shown in the box.

domain is followed by a 23 amino acid hydrophobic transmembrane domain and a 26 amino acid highly charged intracellular domain. There are two potential N-linked glycosylation sites in the extracellular domain. These molecular characteristics are very similar to those seen in human, mouse, and rat Ep-CAM [28–30].

mAb (5-15-1) reacted COS-7 transfected with the cDNA of porcine Ep-CAM

To directly confirm that the antigen of 5-15-1 is porcine Ep-CAM, we generated COS-7 cells transfecting the cDNA of porcine Ep-CAM. For the transfection, we purposely used the pIRES2-EGFP vector system since it is capable, by merit of its containing the IRES sequence, of expressing enhanced GFP (EGFP) and porcine Ep-CAM under one mRNA transcript [34]. The expression plasmid map (pIRES2-EGFP-pEp-CAM) is shown in Fig. 6A. When successfully transfected with pIRES2-EGFP-pEp-CAM, COS-7 cells expressed EGFP and Ep-CAM that could be recognized by 5-15-1 (Fig. 6B). In contrast, COS-7 transfected with an empty vector (pIRES2-EGFP) expressed EGFP but did not react with 5-15-1. These findings demonstrate that 5-15-1 possesses specificity for porcine Ep-CAM.

Expression of Ep-CAM by both IECs and IELs

To definitively prove that Ep-CAM is expressed by both the IECs and IELs of the intestinal epithelium, we performed an immunohistochemical analysis of the intestinal epithelium using FITC-conjugated 5-15-1 specific for Ep-CAM and rhodamine-coupled anti-porcine CD45 mAb together with DAPI counterstaining. The immunohistochemical analysis revealed that Ep-CAM was expressed by IECs and IELs. It is important to note that the expression of Ep-CAM and CD45 were colocalized on the cell surface of IELs (arrowhead in Fig. 7A). In contrast, CD45-positive lymphocytes located in the lamina propria region did not express Ep-CAM (arrow in Fig. 7A). CD45-positive splenocytes also did not react with Ep-CAM-specific mAb 5-15-1 (Fig. 7B). These findings

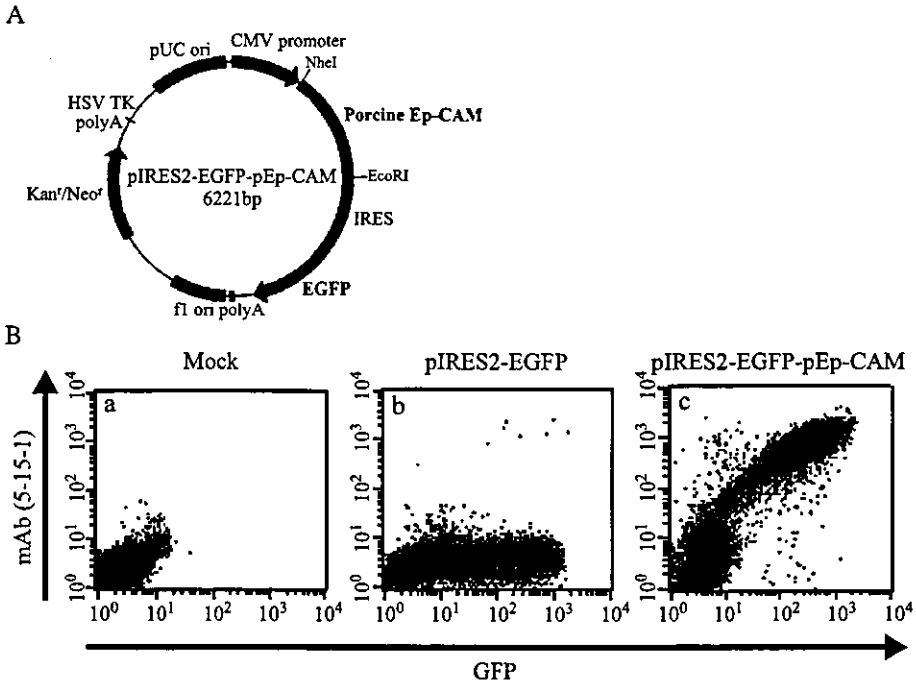

Fig. 6. Ep-CAM-specific 5-15-1 possessed specificity against COS-7 transfected with the cDNA of porcine Ep-CAM. Panel A shows the structure of the porcine Ep-CAM expression plasmid (pIRES2-EGFP-pEP-CAM). This plasmid (pIRES2-EGFP-pEp-CAM) is used for the expression of both porcine Ep-CAM and enhanced GFP (EGFP) because it contains the internal ribosome entry site (IRES). Panel B shows the flow cytometric analysis of nontransfected COS-7 (a), COS-7 transfected with empty vector (pIRES2-EGFP) (b), and pIRES2-EGFP-pEp-CAM (c) by using mAb (5-15-1). mAb (5-15-1) reacted only with COS-7 transfected with pIRES2-EGFP-pEp-CAM (c).

formally demonstrate that Ep-CAM is expressed by both IECs and CD45-positive IELs.

Discussion

The mucosal immune system has been shown to possess several biological characteristics that distinguish it from the systemic immune system [2]. For example, a sheet of intestinal epithelium provides a physical and immunological barrier against invading pathogens by forming an interdependent mucosal intranet between IECs and IELs. One IEL is usually surrounded by six to eight IECs [2]. When γδT cells representing approximately 50% of the murine IELs were removed, epithelial cell growth and MHC class II expression deteriorated [35]. This mutually beneficial relationship between IECs and IELs is reciprocally regulated by a group of mucosal cytokines including IL-7, IL-15, and SCF [17–19]. However, the physical and biological retention mechanism, which maintains IELs in the cellular pocket created by IECs in the intestinal epithelium, still remains unknown. To shed light on this issue, we sought to identify the novel molecule that helps retain IECs and IELs by generating a panel of mAbs specific for the intestinal epithelium. To identify the molecule on the cell surface that allows for physical cross-talk between IECs and IELs, we generated mAbs strongly reactive for the porcine epithelium by immunizing isolated and purified porcine IECs. After splenocytes isolated from immunized Balb/c mice were fused with myeloma (Sp2/0-Ag14), a total of 10 mAb-producing hybridomas were originally generated and screened for their specificity against isolated cells from the porcine intestine using flow cytometry (data not shown). Among these hybridomas, one, designated mAb 5-15-1, was found to strongly react with the basolateral surface of the intestinal epithelium (Fig. 1A). After immunoprecipitation, the antigen of 5-15-1 was detected at a molecular mass of 41–43 kDa by Western blot analysis under nonreducing conditions (Fig. 1B). Furthermore, the antigen was also characterized by using a G.P. Sensor, carbohydrate detection kit (Fig. 1B). Taken together, these data suggest that the surface antigen recognized by mAb 5-15-1 belongs to a family of membrane glycoproteins.

In order to identify the specific antigen of 5-15-1, we next attempted to purify the corresponding molecule from the lysate of the porcine small intestine using affinity chromatography with 5-15-1 (Fig. 4A). When the four major peaks identified by the MALDI-TOF-MS analysis of the purified trypsin-digested antigen (Fig. 4B) were further characterized by tandem MS, one peak was found to match with the peptide sequence of IADVAYYFEK, which corresponds to the human pan-carcinoma antigen epithelial glycoprotein (EGP). EGP was originally identified when various mAbs (e.g., MH99, AUA1, MOC31, 323/A3, KS1/4, GA733, HEA125) were developed and used for the

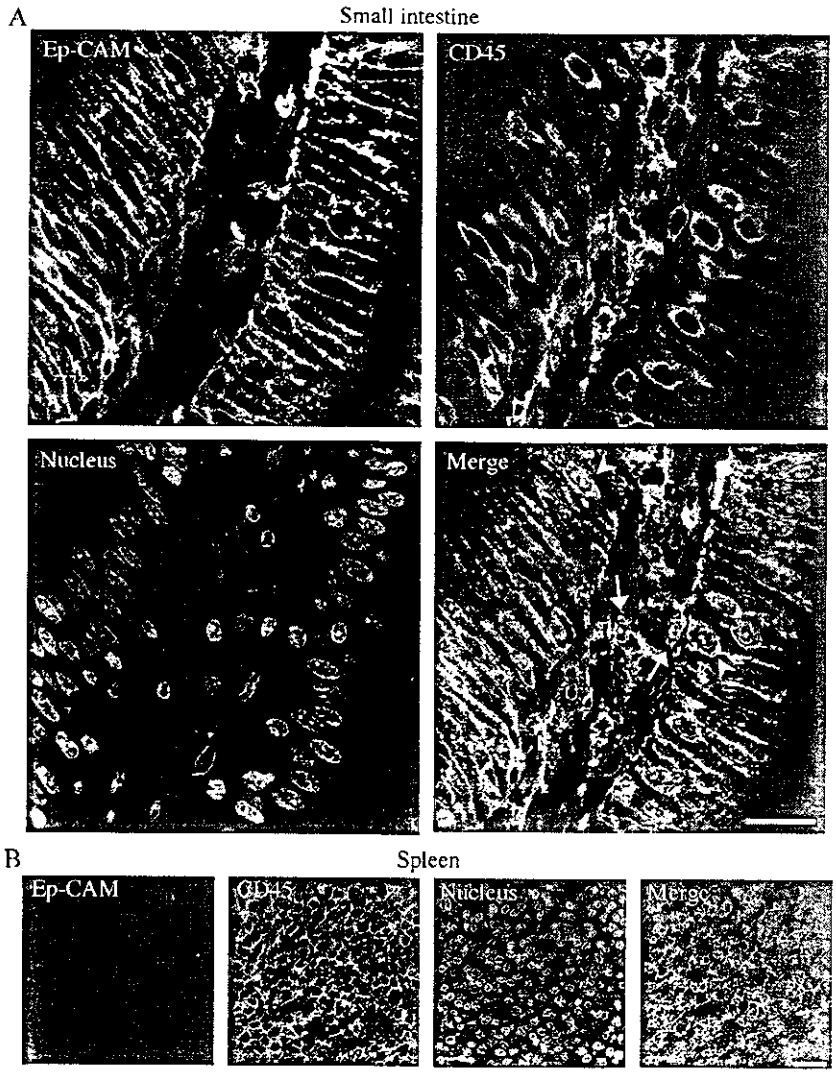

Fig. 7. Double immunohistochemical analysis of porcine small intestine and spleen with mAb 5-15-1 (anti-porcine Ep-CAM) and anti-porcine CD45 mAb. Tissue sections (5 μm) were incubated with anti-porcine Ep-CAM (5-15-1) and anti-porcine CD45 and then stained with FITC-conjugated anti-mouse IgG2b and rhodamine-conjugated anti-mouse IgG1, respectively. The slides were then counterstained by DAPI. In the small intestine, CD45-positive IELs (arrowhead) were costained with anti-porcine Ep-CAM (5-15-1), but such colocalization was not seen for lamina propria lymphocytes (LPLs, arrow) (A). Further, CD45-positive splenocytes did not react with anti-porcine Ep-CAM (5-15-1) (B). Scale bar = 20 μm.

analysis of human epithelial carcinoma [36–41]. Since EGP was initially shown to be expressed by human epithelial carcinoma, the molecule has become the target of EGP-specific immunotherapy and gene therapy strategies [42,43]. However, because EGP is an epithelial differentiation antigen but not a tumor-specific antigen, anti-EGP therapy can cause severe side effects [44]. A few years ago, EGP was shown to be capable of functioning as a Ca^{2+}-independent homophilic cell-to-cell adhesion molecule and received the new designation of epithelial cell adhesion molecule (Ep-CAM) [45,46]. Our present findings further demonstrate the physical homophilic cell-to-cell adhesion capability of Ep-CAM for the formation and maintenance of a sheet-like structure of intestinal epithelium. Thus, E-cadherin was shown to play a crucial role in the maintenance of the intestinal epithelium structure [47]. Ep-CAM may also play a physical role in sustaining the IELs population in the intestinal epithelium since IELs also possess specificity against 5-15-1 (Figs. 3 and 7). Thus, intestinal Ep-CAM is considered to be a key physical retention molecule for IECs and IELs and may provide a first line of defense against mucosal infection. It was recently reported that E-cadherin was recognized as the ligand molecule of internalin expressed by *Listeria monocytogenes* for their invasion to the host [48]. Although we still do not know exact molecular mechanism for the intercellular bacterial entry, Ep-CAM might be target molecule for several micro-organisms to enter the host via the destruction of mucosal epithelium created by IECs and IELs.

Only one of the peaks exhibited the peptide sequence of IADVAYYFEK, which corresponds to Ep-CAM (Fig. 4); the other three peaks identified by MALDI-TOF-MS

analysis were matched with the peptide sequence of actin by the subsequent tandem MS analysis (data not shown). Although the reactivity of 5-15-1 was only confirmed in mucosa-associated epithelium (Figs. 1 and 2), it is well known that anti-actin mAb generally reacts with most eukaryotic cells. Thus, actin is the major protein expressed by all of the mammalian tissues. When we performed the immunohistochemical staining for small intestinal epithelium using 5-15-1 and anti-actin mAb, epithelial cells reacted with both mAbs, as expected (data not shown). A previous study had reported that the cytoplasmic tail of Ep-CAM is capable of associating with the α-actinin [49]. This finding suggests the possibility of a biological association between Ep-CAM and the actin-based cytoskeleton in intestinal epithelial cells. This molecular interaction between the cytoplasmic tail of Ep-CAM and α-actinin has been considered to be a key component of the homophilic adhesion mechanism [49]. These findings lend further credibility to the possibility that the Ep-CAM expressed by both IECs and IELs may behave as a homophilic physical retention molecule for the heterologous cell-to-cell interaction in the intestinal epithelium.

To firmly confirm that 5-15-1 reacted specifically with porcine Ep-CAM, we cloned and sequenced porcine Ep-CAM and then examined the reactivity of 5-15-1 to COS-7 transfected with the isolated cDNA of porcine Ep-CAM (Fig. 6). The cloned cDNA contains an open reading frame (ORF) of 945 bp and encodes for 314 amino acids (Fig. 5). Compared to human, mouse, and rat sequences, the cloned porcine Ep-CAM displayed 71–83% and 77–83% homology at the nucleotide and amino acid levels, respectively (Fig. 5). Based on the characterization and comparison of the sequence with the known Ep-CAM in other species, the cloned porcine Ep-CAM was determined to be a type I transmembrane molecule with 12 conserved cystein residues and at least two N-glycosylation sites, like human, mouse, and rat Ep-CAM. Furthermore, the extracellular domain of porcine Ep-CAM also contained two epidermal growth factor (EGF)-like repeat motifs of $CX_1CX_8CX_7CX_1CX_{10}C$ (position 27-59, EGF-I) and $CX_{32}CX_{10}CX_5CX_1CX_{16}C$ (position 66-135, EGF-II), followed by a cysteine-poor domain (Fig. 5). The Ep-CAM polypeptide was originally shown to consist of 314 amino acids, including a 23 amino acid leader sequence, a 242 amino acid extracellular domain with two EGF-like repeats (EGF-I and EGF-II) within the cystein-rich N-terminal part, a 23 amino acid transmembrane domain, and a 26 amino acid cytoplasmic domain [50]. Among these different sections of the polypeptide, the EGF repeats of the extracellular domain of the Ep-CAM molecule are the most immunodominant epitopes expressed on the cell surface [50,51]. Thus, the focus has been on generating mAbs specific for the EGF-I and -II portion of the Ep-CAM in different species [50,51]. The majority of the currently existing mAbs possess specificity for the first EGF repeat. Based on the Western blot analysis (Fig. 1B), Ep-CAM was detected under nonreducing but not under reducing conditions. These findings suggest that 5-15-1 also recognized the cystein-rich domain of Ep-CAM (e.g., EGF-1, EGF-2). The 5-15-1 specifically reacted with COS-7 cells that had been transfected with the expression plasmid containing the cloned cDNA of porcine Ep-CAM (pIRES2-EGFP-pEp-CAM), but not with the cells transfected with the empty plasmid of pIRES2-EGFP (Fig. 6). Collectively, these results confirm that, by using the newly developed mAb 5-15-1, we have identified the porcine counterpart of Ep-CAM both at the level of the cloned gene and the protein.

It was interesting to note that the expression of 5-15-1 reactive Ep-CAM seemed always to be associated with the presence of IELs in the mucosal epithelium. When 5-15-1 was reacted with several other mucosal tissue-associated epithelial cells in addition to the small intestine (Fig. 2A), epithelial cells in the esophagus and stomach did not react with 5-15-1, while the other mucosa-associated epithelium did and at rates similar to those seen for the small intestinal epithelium. Further, the spleen and liver did not react with 5-15-1. Interestingly, because the esophageal and stomach epithelia are known not to contain IELs [52], they would have no need to express Ep-CAM as the retention molecule between IECs and IELs. Immunoprecipitation and Western blot analysis were used to confirm that all mucosa-associated tissues with the exception of the esophagus and stomach react with 5-15-1 (Fig. 2B). These findings suggest that Ep-CAM is strongly expressed by the mucosal epithelia that are covered by columnar epithelial cells. Since the stomach epithelium has been shown to possess physiological and immunological characteristics that distinguish it from the other mucosa-associated epithelia, its expression of Ep-CAM could be different as well. Taken together with the previous data [41], our current findings suggest that Ep-CAM plays a key role in the physical retention of IECs and IELs in the intestinal epithelium.

Moreover, we used flow cytometry with the appropriate fluorescence-conjugated 5-15-1 to show that Ep-CAM was expressed by IELs but not by splenocytes and PBMCs (Fig. 3). Further, the immunohistochemical analysis indicated that Ep-CAM and CD45 were colocalized on the cell surface of IELs but not of lamina propria lymphocytes (LPLs) (Fig. 7A). These findings further support our contention that a homophilic adhesion molecule of Ep-CAM plays a major biological role in the physical interaction between IECs and IELs. Previous studies reported that $\alpha_E\beta_7$ integrin mediates T cell adhesion to epithelial cells through its binding to E-cadherin, a member of the cadherin family of adhesion molecules that is expressed selectively on epithelial cells [53–55]. In fact, IELs decreased in number but did not disappear in α_E integrin-deficient mice [56]. These data suggest the interesting possibility that another adhesion mechanism mediated by Ep-CAM contributes to the formation and maintenance of an intact intestinal epithelium by physically retaining IELs in the cellular pocket created by IECs and may create an environment of mucosal intranet for

the maintenance of immunological homeostasis. In support of this possibility, a previous study reported that Ep-CAM was expressed in murine thymocyte and might contribute to adhesive interactions between thymocytes and thymus epithelial cells [57]. Currently, we are attempting to directly determine the physical adhesion mechanism via Ep-CAM between IECs and IELs by the creation of Ep-CAM-deficient mice.

In summary, we have used the newly generated mAb 5-15-1 to identify Ep-CAM expression by both intestinal intraepithelial lymphocytes and intestinal epithelial cells. The cell surface antigen recognized by 5-15-1 was a glycoprotein of Ep-CAM with a molecular mass of 41–43 kDa. The characterization of 5-15-1 affinity chromatography-purified glycoprotein by the use of MALDI-TOF-MS and tandem MS analyses demonstrated that the antigen was the porcine homologue of the human pan-carcinoma antigen epithelial glycoprotein, known as alias Ep-CAM. The cloning of the 5-15-1 reactive glycoprotein further confirmed the identification of Ep-CAM at the nucleotide and amino acid levels. The specificity of 5-15-1 was formally proved using COS-7 cells transfected with the cDNA of the cloned porcine Ep-CAM. Interestingly, not only IECs but also IELs reacted with 5-15-1. Since our data demonstrate that both IECs and IELs express homophilic adhesion molecules of Ep-CAM, it is plausible that Ep-CAM is an important element of the physical retention network responsible for retaining IECs and IELs in the intestinal epithelium for the generation of innate defense system.

Acknowledgments

This work was supported by grants from CREST, JST, the Ministry of Education, Science, Sports and Cultures, the Ministry of Health and Welfare, and the Health Science Foundation, Japan.

We thank Mr. H. Fujita of Tokyo Shibaura Zouki and Dr. Nakura and his colleagues of Chugai Research Institute for Medical Science for their helpful sampling of the porcine tissues. We thank Mr. S. Watanabe and Ms. T. Kayamori of Hitachi Science Systems for their help in performing the molecular analyses using MALDI-TOF-MS and tandem MS. We also thank Dr. Kimberly McGhee for reading and editing the manuscript.

References

[1] B. Creamer, The turnover of the epithelium of the small intestine, Br. Med. Bull. 23 (1967) 226–230.

[2] J. Mestecky, R.S. Blumberg, H. Kiyono, J.R. McGhee, The mucosal immune system, in: W.E. Paul (Ed.), Fundamental Immunology, fifth ed., Lipponcott Williams & Wilkins, 2003, pp. 965–1020.

[3] M. Furuse, T. Hirase, M. Itoh, A. Nagafuchi, S. Yonemura, S. Tsukita, Occludin: a novel integral membrane protein localizing at tight junctions, J. Cell Biol. 123 (1993) 1777–1788.

[4] M. Furuse, K. Fujita, T. Hiiragi, K. Fujimoto, S. Tsukita, Claudin-1 and -2: novel integral membrane proteins localizing at tight junctions with no sequence similarity to occludin, J. Cell Biol. 141 (1998) 1539–1550.

[5] K. Morita, M. Furuse, K. Fujimoto, S. Tsukita, Claudin multigene family encoding four-transmembrane domain protein components of tight junction strands, Proc. Natl. Acad. Sci. U. S. A. 96 (1999) 511–516.

[6] J.M. Anderson, C.M. Van Itallie, Tight junctions and the molecular basis for regulation of paracellular permeability, Am. J. Physiol. 269 (1995) G467–G475.

[7] E.E. Schneeberger, R.D. Lynch, Structure, function, and regulation of cellular tight junctions, Am. J. Physiol. 262 (1992) L647–L661.

[8] S. Tsukita, M. Furuse, M. Itoh, Multifunctional strands in tight junctions, Nat. Rev., Mol. Cell Biol. 2 (2001) 285–293.

[9] M. Takeichi, Cadherin cell adhesion receptors as a morphogenetic regulator, Science 251 (1991) 1451–1455.

[10] L. Shapiro, A.M. Fannon, P.D. Kwong, A. Thompson, M.S. Lehmann, G. Grubel, J.F. Legrand, J. Als-Nielsen, D.R. Colman, W.A. Hendrickson, Structural basis of cell–cell adhesion by cadherins, Nature 374 (1995) 306–307.

[11] R. Kemler, From cadherins to catenins: cytoplasmic protein interactions and regulation of cell adhesion, Trends Genet. 9 (1993) 317–321.

[12] T. Kucharzik, S.V. Walsh, J. Chen, C.A. Parkos, A. Nusrat, Neutrophil transmigration in inflammatory bowel disease in associated with differential expression of epithelial intercellular junction proteins, Am. J. Pathol. 159 (2001) 2001–2009.

[13] D. Guy-Grand, M. Malassis-Seris, C. Briottet, P. Vassalli, Cytotoxic differentiation of mouse gut thymodependent and independent intraepithelial T lymphocytes is induced locally, J. Exp. Med. 173 (1991) 1549–1552.

[14] A. Hayday, E. Theodoridis, E. Ramsburg, J. Shires, Intraepithelial lymphocytes: exploring the third way in immunology, Nat. Immunol. 2 (2001) 997–1003.

[15] K. Suzuki, T. Oida, H. Hamada, O. Hitotsumatsu, M. Watanabe, T. Hibi, H. Yamamoto, E. Kubota, S. Kaminogawa, H. Ishikawa, Gut cryptpatches: direct evidence of extrathymic anatomical sites for intestinal T lymphopoiesis, Immunity 13 (2000) 691–702.

[16] X. Cao, E.W. Shores, J. Hu-Li, M.R. Anver, B.L. Kelsall, S.M. Russell, J. Drago, M. Noguchi, A. Grinberg, E.T. Bloom, W.E. Paul, S.I. Katz, P.E. Love, W.J. Lenard, Defective lymphoid development in mice lacking expression of the common cytokine receptor gamma chain, Immunity 2 (1995) 223–238.

[17] M. Yamamoto, H. Kiyono, Role of γδ T cells in mucosal intranet, Allergol. Intern. 48 (1999) 1–5.

[18] K. Inagaki-Ohara, H. Nishimura, A. Mitani, Y. Yoshikai, Interleukin-15 preferentially promotes the growth of intestinal intraepithelial lymphocytes bearing γδ T cell receptor, Eur. J. Immunol. 27 (1997) 2885–2891.

[19] L. Puddington, S. Olson, L. Lefrancois, Interactions between stem cell factor and c-Kit are required for intestinal immune system homeostasis, Immunity 1 (1994) 733–739.

[20] K. Fujihashi, J.R. McGhee, M. Yamamoto, J.J. Peschon, H. Kiyono, An interleukin-7 Internet for intestinal intraepithelial T cell development: knockout of ligand or receptor reveal differences in the immunodeficient state, Eur. J. Immunol. 27 (1997) 2133–2138.

[21] K. Fujihashi, S. Kawabata, T. Hiroi, M. Yamamoto, J.R. McGhee, S. Nisikawa, H. Kiyono, Interleukin 2 (IL-2) and interleukin 7 (IL-7) reciprocally induce IL-7 and IL-2 receptors on gamma delta T-cell receptor-positive intraepithelial lymphocytes, Proc. Natl. Acad. Sci. U. S. A. 93 (1996) 3613–3618.

[22] T. Waldmann, Y. Tagaya, The multifaceted regulation of interleukin-15 expression and the role of this cytokine in NK cell differentiation and host response to intracellular pathogens, Annu. Rev. Immunol. 17 (1999) 19–49.

[23] K. Hirose, H. Suzuki, H. Nishimura, A. Mitani, J. Washizu, T. Matsuguchi, Y. Yoshikai, Interleukin-15 may be responsible for early